Table 1. The clinical characteristics of patients with Reiter's syndrome following intravesical BCG therapy

Case number	Age/sex	No. of BCG therapies	Arthritis	HLA-B27	Therapy	Reference
1	74/M	6	Knees, ankle	−	NSAID	9
2	64/F	4	Elbow, wrist, MCPs, PIPs, knee	+	NSAID + PSL + INH + RFP	10
3	35/F	5	Wrist, MCP, knee	−	NSAID	11
4	68/M	6	Knee	?	INH	12
5	71/F	4	MCP, knee	+	NSAID + PSL + INH	13
6	65/M	5	Elbow, PIP, ankle	+	NSAID + PSL	14
Present case	79/M	4	Shoulder, wrists, MCPs, knees	−	NSAID + PSL	
Present case	54/M	4	Knee	−	PSL	
Present case	58/F	3	Rib, MTP	−	NSAID	
Present case	68/F	5	Rib, knees	?	NSAID	
Present case	47/M	8	Wrist, MCP, knee	−	PSL	
Present case	42/M	6	Knee, PIPs	−	PSL	

BCG, bacillus Calmette–Guérin; MCP, metacarpophalangeal joints; MTP, metatarsophalangeal joints; PIP, proximal interphalangeal joints; PSL, prednisolone; NSAID, nonsteroidal anti-inflammatory drug; INH, isoniazid; RFP, refampicin

such as polyarthritis and conjunctivitis, may be induced. One possible mechanism for this condition is molecular mimicry between BCG and chondrocytes or conjunctiva, which is considered to be important in adjuvant arthritis[4] and Poncet's disease.[5] Adjuvant arthritis is induced in animals by the inoculation of a mycobacterium suspension (Freund). Similarly, Poncet's disease is characterized by an aseptic polyarthritis in association with *Mycobacterium tuberculosis* infection. T cell clones specific for *M. tuberculosis* established from rats with adjuvant arthritis are strongly arthritogenic,[6] suggesting the existence of a cross-reaction between some T cell antigens in human cartilage and *M. tuberculosis*.[7] One of the T cell antigens in the synovial fluid of patients with chronic inflammatory arthritis is a heat-shock protein (HSP) derived from *Mycobacterium bovis*.[8] A relationship between HSP and HSP-specific cytotoxic T cells has been implicated as the possible mechanism of inflammatory responses in patients with Reiter's syndrome.

A Medline search for the period between 1990 and 2002 showed reports of 36 patients with reactive arthritis and 6 patients with Reiter's syndrome that occurred subsequent to intracavitary BCG administration[9–14] (Table 1). Reiter's syndrome was diagnosed based on polyarthritis, aseptic urethritis, and conjunctivitis. These six patients developed asymmetrical arthritis, especially in the knee joints, after four to six doses of BCG immunotherapy. Reiter's syndrome occurred in 6 (7.6%) of 79 patients who received intravesical BCG immunotherapy in our hospital in the 13 years from 1989 to 2002 (Table 2). Three of 10 patients (2 patients were unknown) with BCG-induced Reiter's syndrome were HLA-B27-positive. It is possible that a restricted T cell epitope specific for the HLA-B27 molecule may induce arthrogenic T cells. However, this is not likely in our five patients, because they were negative for the HLA-B27 antigen. Other HLA-B antigens might induce arthrogenic T cells because three of our patients were HLA-B61-positive, two were HLA-B46 positive, and one was HLA-B39-positive. HLA-B39 and B27 recognize an overlapping peptide.[15]

Table 2. Laboratory tests of patients with Reiter's syndrome following intravesical BCG therapy

Case number	Age/sex	CRP (mg/dl)	ESR (mm/h)	ANA	RF
Case 1	79/M	11.3	106	+	−
Case 2	54/M	11.5	56	−	−
Case 3	58/F	1.8	82	−	−
Case 4	68/F	<0.3	ND	ND	ND
Case 5	47/M	1.2	48	−	−
Case 6	42/M	3.8	ND	−	−

CRP, C-reactive protein; ESR, erythrocyte sedimentation rate; ANA, antinuclear antibodies; RF, rheumatoid factor; ND, not done

Our six patients developed Reiter's syndrome after intravesical BCG immunotherapy. Bilateral conjunctivitis and urinary complaints accompanied the occurrence of arthritis. Disorders such as connective tissue disease, septic or microcrystalline arthritis, arthritis secondary to other infectious agents, and seronegative spondyloarthropathy were ruled out by clinical and laboratory findings. Two of our patients responded to treatment with nonsteroidal anti-inflammatory drugs (NSAID), and the other four required steroids. A review of previously reported cases showed that six patients had also had good prognosis and responded favorably to NSAIDs, NSAIDs plus steroids, or antituberculous drugs.

The frequent use of intracavitary BCG may increase the incidence of BCG-induced Reiter's syndrome in the future. The prophylactic administration of isoniazid can prevent adverse effects after BCG therapy, but animal studies[16] suggest that prophylactic antituberculous drug therapy can reduce the antitumor effect as well as the immune response. Immunological studies are needed to determine the underlying pathogenic mechanism(s) of arthritis and conjunctivitis, and to search for an effective treatment or prevention of adverse events after intracavitary BCG immunotherapy.

References

1. Morales A, Eidinger D, Bruce AW. Intracavitary bacillus Calmette-Guerin in the treatment of superficial bladder tumors. J Urol 1976;116:180–3.
2. Lamm DL, Stogdill VD, Stogdill BJ, Crispen RG. Complications of bacillus Calmette-Guerin immunotherapy in 1278 patients with bladder cancer. J Urol 1986;135:272–4.
3. Hughes RA, Allard SA, Maini RN. Arthritis associated with adjuvant mycobacterial treatment for carcinoma of the bladder. Ann Rheum Dis 1988;48:432–4.
4. Pearson CM. Experimental models in rheumatoid disease. Arthritis Rheum 1964;7:80–6.
5. Dall L, Long L, Stanford J. Poncet's disease: tuberculous rheumatism. Rev Infect Dis 1989;11:105–7.
6. Holoshitz J, Matitiau A, Cohen IR. Arthritis induced in rats by cloned T lymphocytes responsive to mycobacteria but not to collagen type II. J Clin Invest 1984;73:211–5.
7. van Eden W, Holoshitz J, Nevo Z, Frenkel A, Klajman A, Cohen IR. Arthritis induced by a T-lymphocyte clone that responds to *Mycobacterium tuberculosis* and to cartilage proteoglycans. Proc Natl Acad Sci USA 1985;82:5117–20.
8. Res PC, Schaar CG, Breedveld FC, van Eden W, van Embden JD, Cohen IR, et al. Synovial fluid T cell reactivity against 65-kD heatshock protein of mycobacteria in early chronic arthritis. Lancet 1988;2:478–80.
9. Faus S, Martinez Montauti JM, Puig L. Reiter's syndrome after administration of intravesical bacille Calmette-Guerin. Clin Infect Dis 1993;17:526–7.
10. Pancaldi P, Van Linthoudt D, Alborino D, Haefliger JM, Ott H. Reiter's syndrome after intravesical bacillus Calmette-Guerin treatment for superficial bladder carcinoma. Br J Rheumatol 1993;32:1096–8.
11. Saporta L, Gumus E, Karadag H, Kuran B, Miroglu C. Reiter syndrome following intracavitary BCG administration. Scand J Urol Nephrol 1997;31:211–2.
12. Hansen CP, Mortensen S. Epididymo-orchitis and Reiter's disease. Two infrequent complications after intravesical bacillus Calmette-Guerin therapy. Scand J Urol Nephrol 1997;31:317–8.
13. Hogarth MB, Thomas S, Seifert MH, Tariq SM. Reiter's syndrome following intravesical BCG immunotherapy. Postgrad Med J 2000;76:791–3.
14. Hodish I, Ezra D, Gur H, Strugo R, Olchovsky D. Reiter's syndrome after intravesical bacillus Calmette-Guerin therapy for bladder cancer. Isr Med Assoc J 2000;2:240–1.
15. Sobao Y, Tsuchiya N, Takiguchi M, Tokunaga K. Overlapping peptide binding specificities of HLA-B27 and B39: evidence for a role of peptide supermotif in the pathogenesis of spondyloarthropathies. Arthritis Rheum 1999;42:175–81.
16. De Boer LC, Steerenberg PA, Van der Meijden PM, Van Klingeren B, De Jong WH, Elgersma A, et al. Impaired immune response by isoniazid treatment during intravesical BCG administration in the guinea pig. J Urol 1992;148:1577–82.

ARTHRITIS & RHEUMATISM
Vol. 52, No. 1, January 2005, pp 212–218
DOI 10.1002/art.20741

Significance of Valine/Leucine^{247} Polymorphism of β_2-Glycoprotein I in Antiphospholipid Syndrome

Increased Reactivity of Anti–β_2-Glycoprotein I Autoantibodies to the Valine^{247} β_2-Glycoprotein I Variant

Shinsuke Yasuda,[1] Tatsuya Atsumi,[1] Eiji Matsuura,[2] Keiko Kaihara,[2] Daisuke Yamamoto,[3] Kenji Ichikawa,[1] and Takao Koike[1]

Objective. To clarify the consequences of the valine/leucine polymorphism at position 247 of the β_2-glycoprotein I (β_2GPI) gene in patients with antiphospholipid syndrome (APS), by investigating the correlation between genotypes and the presence of anti-β_2GPI antibody. The reactivity of anti-β_2GPI antibodies was characterized using recombinant Val^{247} and Leu^{247} β_2GPI.

Methods. Sixty-five Japanese patients with APS and/or systemic lupus erythematosus who were positive for antiphospholipid antibodies and 61 controls were analyzed for the presence of the Val/Leu^{247} polymorphism of β_2GPI. Polymorphism assignment was determined by polymerase chain reaction followed by restriction enzyme digestion. Recombinant Val^{247} and Leu^{247} β_2GPI were established to compare the reactivity of anti-β_2GPI antibodies to β_2GPI between these variants. The variants were prepared on polyoxygenated plates or cardiolipin-coated plates, and the reactivity of a series of anti-β_2GPI antibodies (immunized anti-human β_2GPI monoclonal antibodies [Cof-19–21] and autoimmune anti-β_2GPI monoclonal antibodies [EY1C8, EY2C9, and TM1G2]) and IgGs purified from patient sera was investigated.

Results. A positive correlation between the Val^{247} allele and the presence of anti-β_2GPI antibodies was observed in the patient group. Human monoclonal/polyclonal anti-β_2GPI autoantibodies showed higher binding to recombinant Val^{247} β_2GPI than to Leu^{247} β_2GPI, although no difference in the reactivity of the immunized anti-β_2GPI between these variants was observed. Conformational optimization showed that the replacement of Leu^{247} by Val^{247} led to a significant alteration in the tertiary structure of domain V and/or the domain IV–V interaction.

Conclusion. The Val^{247} β_2GPI allele was associated with both a high frequency of anti-β_2GPI antibodies and stronger reactivity with anti-β_2GPI antibodies compared with the Leu^{247} β_2GPI allele, suggesting that the Val^{247} β_2GPI allele may be one of the genetic risk factors for development of APS.

The antiphospholipid syndrome (APS) is characterized by arterial/venous thrombosis and pregnancy morbidity in the presence of antiphospholipid antibodies (aPL) (1–3). Among the targets of aPL, β_2-glycoprotein I (β_2GPI), which bears epitopes for anticardiolipin antibodies (aCL), has been extensively studied (4–6). APS-related aCL do not recognize free β_2GPI, but do recognize β_2GPI when it is complexed with phospholipids or negatively charged surfaces, by exposure of cryptic epitopes (7) or increment of antigen density (8).

The significance of antigen polymorphism in the production of autoantibodies or the development of autoimmune diseases is now being widely discussed. It is speculated that amino acid substitution in antigens can lead to differences in antigenic epitopes of a given protein. In particular, β_2GPI undergoes conformational

[1]Shinsuke Yasuda, MD, PhD, Tatsuya Atsumi, MD, PhD, Kenji Ichikawa, MD, PhD, Takao Koike, MD, PhD: Hokkaido University Graduate School of Medicine, Sapporo, Japan; [2]Eiji Matsuura, PhD, Keiko Kaihara, PhD: Okayama University Graduate School of Medicine, Okayama, Japan; [3]Daisuke Yamamoto, MD, PhD: Osaka Medical College, Takatsuki, Japan.

Address correspondence and reprint requests to Tatsuya Atsumi, MD, PhD, Medicine II, Hokkaido University Graduate School of Medicine, N15 W7, Kita-ku, Sapporo 060-8638, Japan. E-mail: at3tat@med.hokudai.ac.jp.

Submitted for publication May 10, 2004; accepted in revised form September 27, 2004.

alteration upon interaction with phospholipids (9). β_2GPI polymorphism on or near the phospholipid binding site can affect the binding or production of aCL (anti-β_2GPI autoantibodies), the result being altered development of APS. Polymorphism near the antigenic site, or which leads to alteration of the tertiary structure of the whole molecule, may affect the binding of autoantibodies. Five different gene polymorphisms of β_2GPI attributable to a single-nucleotide mutation have been described: 4 are a single amino acid substitution at positions 88, 247, 306, and 316 (10), and the other is a frameshift mutation associated with β_2GPI deficiency found in the Japanese population (11). In particular, the Val/Leu^{247} polymorphism locates in domain V of β_2GPI, between the phospholipid binding site in domain V and the potential epitopes of anti-β_2GPI antibodies in domain IV, as we reported previously (12). Although anti-β_2GPI antibodies are reported to direct to domain I (13) or domain V (14) as well, it should be considered that a certain polymorphism alters the conformation of the molecule, affecting function or antibody binding at a distant site.

We previously reported that, in a group of British Caucasian subjects, the Val^{247} allele was significantly more frequent in primary APS patients with anti-β_2GPI antibodies than in controls or in primary APS patients without anti-β_2GPI antibodies (15), but the importance of the Val^{247} allele in patients with APS is still controversial. In this study, we analyzed the correlation between the β_2GPI Val^{247} allele and anti-β_2GPI antibodies in the Japanese population. We also investigated the reactivity of anti-β_2GPI antibodies to recombinant Val^{247} β_2GPI and Leu^{247} β_2GPI, using a series of monoclonal anti-β_2GPI antibodies and IgGs purified from sera of patients with APS. Finally, to investigate the difference in anti-β_2GPI binding to those variants, we conformationally optimized to domain V and the domain IV–V complex of β_2GPI variants at position 247, referring the crystal structure of β_2GPI.

PATIENTS AND METHODS

Patients and controls. The study group comprised 65 patients (median age 38 years [range 18–74 years]; 57 women and 8 men) who attended the Hokkaido University Hospital, all of whom were positive for aPL (IgG, IgA, or IgM class aCL, and/or lupus anticoagulant). Thirty-four patients had APS (16 had primary APS, and 18 had secondary APS), and 31 patients did not have APS (24 had systemic lupus erythematosus [SLE], and 7 had other rheumatic diseases). Among all subjects, 19 had a history of arterial thrombosis, and 6 had venous thrombosis. Of the 31 patients with a history of pregnancy, 8 experienced pregnancy complications (some patients had more than 1 manifestation of pregnancy morbidity). Anti-β_2GPI antibodies were detected by enzyme-linked immunosorbent assay (ELISA) as β_2GPI-dependent aCL (16). IgG, IgA, or IgM class β_2GPI-dependent aCL were found in 30, 14, and 21 patients, respectively (some patients had >1 isotype), and 34 patients had at least 1 of those isotypes. Lupus anticoagulant, detected by 3 standard methods described previously (17), was found in 51 patients. The diagnoses of APS and SLE, respectively, were based on the preliminary classification criteria for definite APS (18) and the American College of Rheumatology criteria for the classification of SLE (19). Informed consent was obtained from each patient or control subject. The control group comprised 61 healthy individuals with no history of autoimmune, thrombotic, or notable infectious disease.

Determination of β_2GPI gene polymorphism. Genomic DNA was extracted from peripheral blood mononuclear cells (PBMCs) using a standard phenol–chloroform extraction procedure or the DnaQuick kit (Dainippon, Osaka, Japan). Polymorphism assignment was determined by polymerase chain reaction (PCR) followed by allele-specific restriction enzyme digestion (PCR–restriction fragment length polymorphism) using *Rsa* I (Promega, Southampton, UK) as described previously (15).

Purification of patient IgG. Sera from 11 patients positive for IgG class β_2GPI-dependent aCL were collected. The mean (±SD) titer of aCL IgG from these patients was 29.0 ± 21.5 IgG phospholipid (GPL) units (range 12.4 to >98 GPL units). IgG was purified from these sera using a protein G column and the MAbTrap GII IgG purification kit (Pharmacia Biotech, Freiburg, Germany), as recommended by the manufacturer.

Monoclonal anti-β_2GPI antibodies. Two types of anti-β_2GPI monoclonal antibodies were used. Cof-19, Cof-20, and Cof-21 are mouse monoclonal anti-human β_2GPI antibodies obtained from immunized BALB/c mice, directed to domains V, III, and IV of β_2GPI, respectively. These monoclonal antibodies recognize the native structure of human β_2GPI (12).

EY1C8, EY2C9, and TM1G2 are IgM class autoimmune monoclonal antibodies established from patients with APS (20). These antibodies bind to domain IV of β_2GPI, but only after interaction with solid-phase phospholipids or with a polyoxygenated polystyrene surface. EY1C8 and EY2C9 were established from a patient whose genotype of β_2GPI was heterozygous for Val/Leu^{247}. The genotype of the patient with TM1G2 was not determined.

Preparation of recombinant β_2GPI. As previously reported, genes were expressed in *Spodoptera frugiperda* Sf9 insect cells infected with recombinant baculoviruses (12). A full-length complementary DNA of human β_2GPI coding Val^{247} was originally obtained from Hep-G2 cells (21), and the valine residue was replaced by leucine, using the GeneEditor in vitro Site-Directed Mutagenesis System (Promega, Madison, WI). The sequence of the primers for a mutant Val^{247}→Leu (GTA→TTA) is as follows: 5′-GCATCTTGTAAATTACCTGTGAAAAAAG-3′. A DNA sequence of the mutant was verified by analysis using ABI Prism model 310 (PE Applied Biosystems, Foster City, CA).

Binding assays of monoclonal anti-β_2GPI antibodies and purified IgGs to the recombinant β_2GPI (cardiolipin-coated plate). The reactivity of a series of monoclonal anti-β_2GPI antibodies and IgG fractions (purified from the sera of APS patients positive for IgG class anti-β_2GPI) against 2 β_2GPI variants was investigated using an ELISA. ELISAs were performed using a cardiolipin-coated plate as previously reported (16) but with a slight modification. Briefly, the wells of Sumilon Type S microtiter plates (Sumitomo Bakelite, Tokyo, Japan) were filled with 30 μl of 50 μg/ml cardiolipin (Sigma, St. Louis, MO) and dried overnight at 4°C. After blocking with 2% gelatin in phosphate buffered saline (PBS) for 2 hours and washing 3 times with 0.05% PBS–Tween, 50 μl of 10 μg/ml recombinant β_2GPI and controls were distributed and incubated for 30 minutes at room temperature. Wells were filled with 50 μl of serial dilutions of monoclonal antibodies (Cof-19–21, EY1C8 and EY2C9, and TM1G2) or purified patient IgG (100 μg/ml), followed by incubation for 30 minutes at room temperature. After washing 3 times, 50 μl of alkaline phosphatase–conjugated anti-mouse IgG (1:3,000), anti-human IgM (1:1,000), or anti-human IgG (1:6,000) was distributed and incubated for 1 hour at room temperature. The plates were washed 4 times, and 100 μl of 1 mg/ml *p*-nitrophenyl phosphate disodium (Sigma) in 1*M* diethanolamine buffer (pH 9.8) was distributed. Optical density (OD) was read at 405 nm, with reference at 620 nm. One percent fatty acid–free bovine serum albumin (BSA) (A-6003; Sigma)–PBS was used as sample diluent and control.

Binding assays of monoclonal anti-β_2GPI antibodies to recombinant β_2GPI (polyoxygenated plate). Anti-β_2GPI antibody detection assay using polyoxygenated plates was performed as previously reported (22), with minor modifications. Briefly, the wells of polyoxygenated MaxiSorp microtiter plates (Nalge Nunc International, Roskilde, Denmark) were coated with 50 μl of 1 μg/ml recombinant β_2GPI in PBS and incubated overnight at 4°C. After blocking with 3% gelatin–PBS at 37°C for 1 hour and washing 3 times with PBS–Tween, 50 μl of monoclonal antibodies, diluted with 1% BSA–PBS, were distributed and incubated for 1 hour at room temperature. The following steps were taken, in a similar manner.

Conformational optimization of domain V and the domain IV–V complex in human β_2GPI variants at position 247. A conformation of domain V in the valine variant at position 247 was first constructed from the crystal structure of the leucine variant (implemented in Protein Data Bank: 1C1Z) (23). Replacement of leucine by valine at position 247 was performed using the Quanta system (Molecular Simulations, San Diego, CA), and the model was optimized by 500 cycles of energy minimization by the CHARMm program (24), with hydrophilic hydrogen atoms and TIP3 water molecules (25). Molecular dynamics simulation (5 psec) of the model was then performed with 0.002 psec time steps. The cutoff distance for nonbonded interactions was set to 15Å, and the dielectric constant was 1.0. A nonbonded pair list was updated every 10 steps. The most stable structure of each domain in the dynamics iterations was then optimized by 500 cycles of energy minimization. The final structures of domain V consisted of 2,616 atoms, including 603 TIP3 water molecules, and had a total energy of -1.63×10^4 kcal/mole with a root-mean-square force of 0.869 kcal/mole.

Molecular models of a domain IV–V complex (leucine and valine variants at position 247) were further constructed by considering the location of the oligosaccharide attachment site in domain IV, the location of epitopic regions of the Cof-8 and Cof-20 monoclonal antibodies, the junction between domains IV and V, and molecular surface charges of both domains. These models were again optimized by molecular dynamics simulation and by energy minimization as described above. The final structures of the complex in the leucine and valine variants consisted of 3,773 and 3,778 atoms, respectively, including hydrophilic hydrogen atoms and 806 and 808 TIP3 water molecules, respectively, and had total energy of -2.07×10^4 and -2.03×10^4 kcal/mole with a root-mean-square force of 0.985 and 0.979 kcal/mole, respectively.

Statistical analysis. Correlations between the allele frequencies and clinical features such as the positiveness of β_2GPI-dependent aCL were expressed as odds ratios (ORs) and 95% confidence intervals (95% CIs). *P* values were determined by chi-square test with Yates' correction. *P* values less than or equal to 0.05 were considered significant.

RESULTS

Val/Leu^{247} polymorphism of β_2GPI and the presence of β_2GPI-dependent aCL. As shown in Table 1, the Leu^{247} allele was dominant in the population of healthy Japanese individuals, compared with Caucasians, which is consistent with a previous report (26). Japanese patients with anti-β_2GPI had a significantly increased frequency of the Val^{247} allele, compared with Japanese patients without anti-β_2GPI ($P = 0.0107$) or Japanese controls ($P = 0.0209$).

The binding of autoimmune anti-β_2GPI to recombinant Val^{247} and Leu^{247} β_2GPI. Representative binding curves using cardiolipin-coated plates and polyoxygenated plates are shown in Figure 1. Regardless of the type of plates, Cof-20 bound equally to valine and leucine variants of β_2GPI (Figures 1a and c), in any concentration of Cof-20. The binding curves of Cof-19 and Cof-21 were similar to that of Cof-20 (results not

Table 1. Frequency of the Val^{247} allele of β_2GPI in patients with APS*

Group	Japanese	British Caucasians
Patients with anti-β_2GPI	23/68 (33.8)†	48/56 (85.7)‡
Patients without anti-β_2GPI	9/62 (14.5)	39/58 (67.2)
Controls	23/122 (18.9)	55/78 (70.5)

* Values are the number (%). β_2GPI = β_2-glycoprotein I; APS = antiphospholipid syndrome.
† $P = 0.0107$ versus patients without anti-β_2GPI (odds ratio [OR] 3.01, 95% confidence interval [95% CI] 1.26–7.16), and $P = 0.0209$ versus controls, by chi-square test (OR 2.15, 95% CI 1.09–4.23).
‡ $P = 0.204$ versus patients without anti-β_2GPI (OR 2.92, 95% CI 1.16–7.39), and $P = 0.0396$ versus controls, by chi-square test (OR 2.51, 95% CI 1.03–6.13).

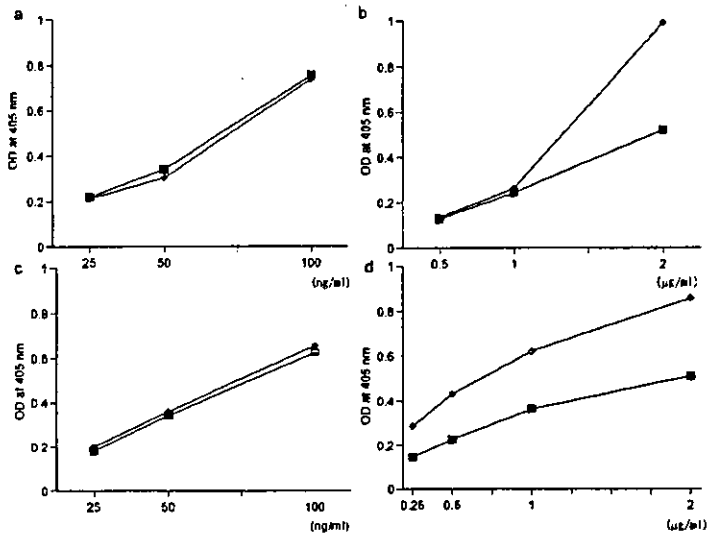

Figure 1. Representative binding curves of monoclonal anti-β_2-glycoprotein I (anti-β_2GPI) antibodies to recombinant valine/leucine^{247} β_2GPI. **a**, Binding curve of Cof-20 using cardiolipin-coated plate. **b**, Binding curve of EY2C9 using cardiolipin-coated plate. **c**, Binding curve of Cof-20 using polyoxygenated plate. **d**, Binding curve of EY2C9 using polyoxygenated plate. Binding to Val^{247} β_2GPI and Leu^{247} β_2GPI are indicated with diamonds and squares, respectively. OD = optical density.

shown). In contrast, EY2C9 showed stronger binding to Val^{247} β_2GPI than to Leu^{247} β_2GPI (Figures 1b and d). EY1C8 and TM1G2 also showed stronger binding to Val^{247} β_2GPI. Figure 2a shows the binding of the monoclonal antibodies, on cardiolipin-coated plates, in the following concentrations: for Cof-19–21, 100 ng/ml;

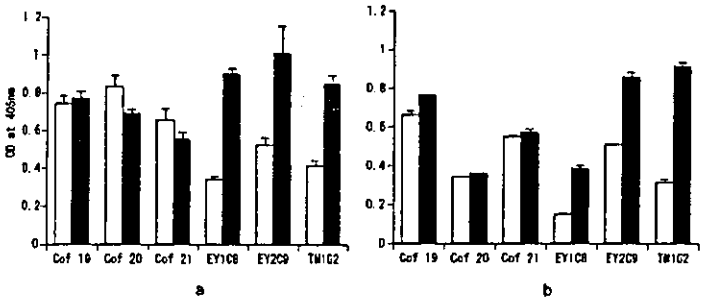

Figure 2. Reactivity of anti-β_2-glycoprotein I (anti-β_2GPI) antibodies to β_2GPI variants. **a**, The binding of monoclonal anti-β_2GPI antibodies to the recombinant valine/leucine^{247} β_2GPI was investigated using enzyme-linked immunosorbent assay (ELISA) on cardiolipin-coated plates. Concentrations of antigens and antibodies were as follows: for recombinant β_2GPI, 10 μg/ml; for Cof-19–21, 100 ng/ml; for EY1C8 and EY2C9, 2 μg/ml; for TM1G2, 5 μg/ml. **b**, The binding of monoclonal anti-β_2GPI antibodies to the recombinant Val/Leu^{247} β_2GPI was investigated using ELISA on polyoxygenated plates. Concentrations of antigens and antibodies were as follows: for recombinant β_2GPI, 1 μg/ml; for Cof-19–21, 50 ng/ml; for EY1C8 and EY2C9, 2 μg/ml; for TM1G2, 5 μg/ml. Results were presented as the optical density (OD) at 405 nm. Open columns indicate binding activity to Leu^{247} β_2GPI, and solid columns indicate binding activity to Val^{247} β_2GPI. Bars show the mean and SD.

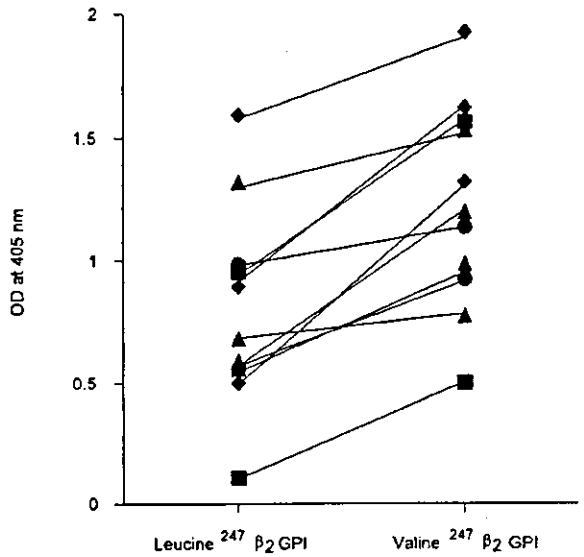

Figure 3. Reactivity of purified IgG from patients (100 μg/ml) to recombinant Val/Leu^{247} β_2-glycoprotein I (β_2GPI) (10 μg/ml), presented as the optical density (OD) at 405 nm. Squares, circles, and triangles indicate patients homozygous for the Leu^{247} allele, homozygous for the Val^{247} allele, and heterozygous for the Val/Leu^{247} allele, respectively. Diamonds indicate patients whose genotypes were not available.

for EY1C8 and EY2C9, 1 μg/ml; and for TM1G2, 2.5μg/ml. In contrast with the close reactivity of Cof-19, Cof-20, and Cof-21 between Val^{247} β_2GPI and Leu^{247} β_2GPI, autoimmune monoclonal antibodies (EY1C8, EY2C9, and TM1G2) showed higher binding to Val^{247} β_2GPI than to Leu^{247} β_2GPI. The autoimmune monoclonal antibodies also showed a higher binding to Val^{247} β_2GPI directly coated on polyoxygenated plates (Figure 2b). IgG in sera collected from 11 patients (100 μg/ml) also showed higher binding to Val^{247} β_2GPI than to Leu^{247} β_2GPI on cardiolipin-coated plates, regardless of the patients' genotypes (Figure 3).

Conformational alteration by leucine replacement by valine at position 247. Each domain V conformation in 2 variants at position 247 is shown in Figure 4a. The root-mean-square deviations for matching backbone atoms and equivalent atoms in the leucine and valine variants were 0.76 and 1.11 Å, respectively. The largest shift was observed at Val^{305}, one of the residues located on the backbone neighboring position 247. The shift seemed to be caused by weak flexibility of side chains consisting of Val^{247}, Pro^{248}, and Val^{249} and the electrostatic interactions between Lys^{250}, Lys^{251}, Glu^{307} and Lys^{308}.

The molecular models of the IV–V complex in leucine and valine variants are shown in Figure 4b. The root-mean-square deviations for matching these backbone atoms and equivalent atoms were 1.72 and 2.03 Å, respectively. Electrostatic interactions and hydrogen bonds between Asp^{193} and Lys^{240}/Lys^{250}, Asp^{222} and Lys^{305}, and Glu^{228} and Lys^{308} appeared in the IV–V complex, but the interaction between Glu^{228} and Lys^{308} was disrupted by the leucine replacement by valine, because direction of the Lys^{308} side chain was significantly changed in the complex. As a result, Trp^{235} of domain IV, located on the contact surface with domain V, was slightly shifted.

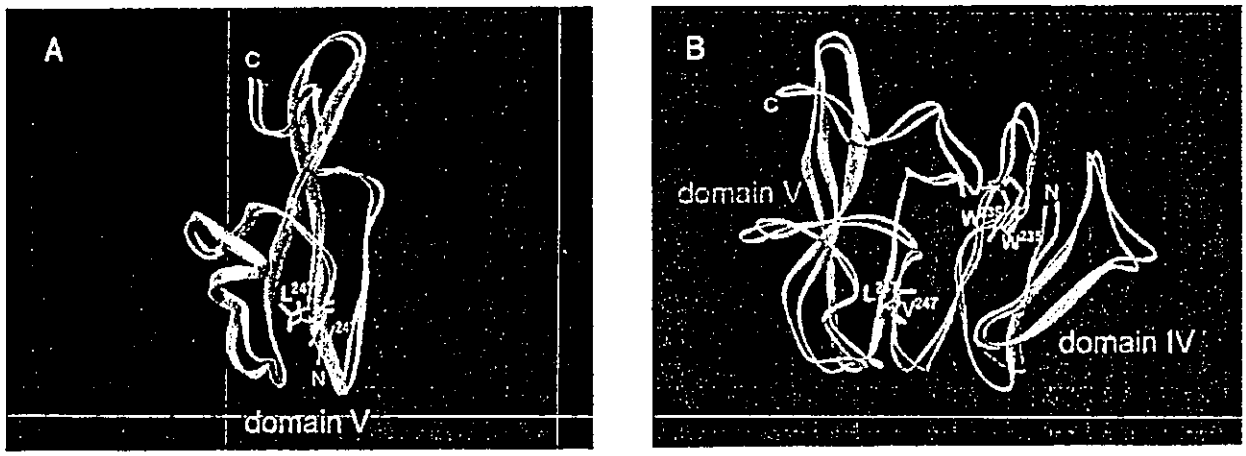

Figure 4. Conformational alterations in domain V (A) and in the domain IV–V complex (B), replacing leucine by valine at position 247. Structure of the valine (light blue) and leucine (white) variants was shown by a ribbon representation with the secondary structure.

DISCUSSION

This study shows the positive correlation between the Val^{247} β_2GPI allele and anti-β_2GPI antibody production in a Japanese population, confirming the correlation observed in a British Caucasian population in our previous report (15). A positive correlation between the Val^{247} allele and the presence of anti-β_2GPI antibodies was also reported in Asian American (26) and Mexican patients (27). However, this correlation was not observed in other American populations (26) or in patients with thrombosis or pregnancy complications in the UK (28). This discrepancy may be the result of the difference in the frequency of the Val^{247} allele among races, or the difference in the background of investigated patients. Another possibility is that the relationship between the Val^{247} allele and thrombosis in Caucasians may be controversial due to underpowered studies or to differences in the procedure used to detect anti-β_2GPI antibodies. Methods for the detection of anti-β_2GPI antibodies differ among laboratories. For example, cardiolipin-coated plates or oxygenated plates are used in some methods, whereas unoxygenated plates are used in others. In addition, bovine β_2GPI is used instead of human β_2GPI in some assays. The antibodies used for standardization also differ, although monoclonal antibodies such as EY2C9 and HCAL (29) have been proposed as international standards of calibration materials.

β_2GPI is a major target antigen for aCL, and, according to our previous investigation, B cell epitopes reside in domain IV and are considered to be cryptic and to appear only when β_2GPI interacts with negatively charged surfaces such as cardiolipin, phosphatidylserine, or polyoxygenated polystyrene surface (7), although other studies indicate that the B cell epitopes are located on domain I (13) or domain V (14). According to another interpretation for the specificity of aCL, increment of the local antigen density on the negatively charged surface also contributes to anti-β_2GPI detection in ELISA (8,30). Studies on the crystal structure of human β_2GPI revealed that the lysine-rich site and an extended C-terminal loop region on domain V are crucial for phospholipid binding. Position 247 is located at the N-terminal side of domain V, and, around this position, Lys^{242}, Ala^{243}, and Ser^{244} were suggested to play a role in the interaction between domains IV and V (9,23,31).

Although the Val/Leu^{247} polymorphism may not be very critical for the autoantibody binding, the amino acid substitution at this point was revealed to affect the affinity of monoclonal aCL established from patients with APS and that of purified IgG from patients positive for β_2GPI-dependent aCL. We conformationally optimized to domain V and the domain IV–V complex of β_2GPI variants at position 247, referring the crystal structure of β_2GPI. IgG aCL was screened using the standardized aCL ELISA, in which both the Leu^{247} and the Val^{247} allele of β_2GPI are contained as antigen. Although biochemical characteristics and structure are similar between valine and leucine, the replacement of Leu^{247} by Val^{247} leads to a significant alteration in the tertiary structure of domain V and/or the domain IV–V interaction (Figure 4). It is likely that the structural alteration affects the affinity between anti-β_2GPI autoantibodies and the epitope(s) present on its molecule. One explanation for this phenomenon is that this β_2GPI polymorphism affects the electrostatic interaction between domain IV and domain V or the protein–protein interaction, resulting in differences in the accessibility of the recognition site by the autoantibodies, or the local density of β_2GPI.

Another possible explanation of the correlation between the Val/Leu^{247} polymorphism of β_2GPI and anti-β_2GPI antibodies is T cell reactivity. Ito et al (32) investigated T cell epitopes of patients with anti-β_2GPI autoantibodies by stimulating patients' PBMCs with a peptide library that covers the β_2GPI sequence. Four of 7 established CD4+ T cell clones reacted to peptide fragments that include amino acid position 244–264, then position 247 is included among the candidate epitopes. Arai et al (33) found preferred recognition of peptide position 276–290 by T cell clones from patients with APS. They also found high reactivity to peptide 247–261 in one patient. We speculate that a small alteration in the conformation arising from the valine/leucine substitution at position 247 may affect the susceptibility to generate autoreactive T cell clones in patients with APS.

Our results in this study indicate that the Val/Leu^{247} polymorphism affects the antigenicity of β_2GPI for anti-β_2GPI autoantibodies, and that the Val^{247} allele can be a risk factor for having autoantibodies against this molecule. Therefore, the Val/Leu^{247} variation of β_2GPI may be crucial for autoimmune reactivity against β_2GPI. We further show the significance of the Val/Leu^{247} polymorphism of β_2GPI in the strength of the binding between β_2GPI and anti-β_2GPI autoantibodies. The significance of antigen polymorphisms in the production of autoantibodies or in the development of autoimmune diseases is not well understood. To our knowledge, this report is the first to present a genetic polymorphism of

autoantigen directly affecting its interaction with autoantibodies.

REFERENCES

1. Hughes GR. The antiphospholipid syndrome: ten years on. Lancet 1993;342:341–4.
2. Hughes GR, Harris EN, Gharavi AE. The anticardiolipin syndrome. J Rheumatol 1986;13:486–9.
3. Harris EN, Gharavi AE, Hughes GR. Anti-phospholipid antibodies. Clin Rheum Dis 1985;11:591–609.
4. Galli M, Comfurius P, Maassen C, Hemker HC, de Baets MH, van Breda-Vriesman PJ, et al. Anticardiolipin antibodies (ACA) directed not to cardiolipin but to a plasma protein cofactor. Lancet 1990;335:1544–7.
5. McNeil HP, Simpson RJ, Chesterman CN, Krilis SA. Anti-phospholipid antibodies are directed against a complex antigen that includes a lipid-binding inhibitor of coagulation: β_2-glycoprotein I (apolipoprotein H). Proc Natl Acad Sci U S A 1990;87:4120–4.
6. Matsuura E, Igarashi Y, Fujimoto M, Ichikawa K, Koike T. Anticardiolipin cofactor(s) and differential diagnosis of autoimmune disease. Lancet 1990;336:177–8.
7. Matsuura E, Igarashi Y, Yasuda T, Triplett DA, Koike T. Anticardiolipin antibodies recognize β_2-glycoprotein I structure altered by interacting with an oxygen modified solid phase surface. J Exp Med 1994;179:457–62.
8. Roubey RA, Eisenberg RA, Harper MF, Winfield JB. "Anticardiolipin" autoantibodies recognize β_2-glycoprotein I in the absence of phospholipid: importance of Ag density and bivalent binding. J Immunol 1995;154:954–60.
9. Schwarzenbacher R, Zeth K, Diederichs K, Gries A, Kostner GM, Laggner P, et al. Crystal structure of human β_2-glycoprotein I: implications for phospholipid binding and the antiphospholipid syndrome. EMBO J 1999;18:6228–39.
10. Sanghera DK, Kristensen T, Hamman RF, Kamboh MI. Molecular basis of the apolipoprotein H (β_2-glycoprotein I) protein polymorphism. Hum Genet 1997;100:57–62.
11. Yasuda S, Tsutsumi A, Chiba H, Yanai H, Miyoshi Y, Takeuchi R, et al. β_2-glycoprotein I deficiency: prevalence, genetic background and effects on plasma lipoprotein metabolism and hemostasis. Atherosclerosis 2000;152:337–46.
12. Igarashi M, Matsuura E, Igarashi Y, Nagae H, Ichikawa K, Triplett DA, et al. Human β_2-glycoprotein I as an anticardiolipin cofactor determined using mutants expressed by a baculovirus system. Blood 1996;87:3262–70.
13. Iverson GM, Victoria EJ, Marquis DM. Anti-β_2 glycoprotein I (β_2GPI) autoantibodies recognize an epitope on the first domain of β_2GPI. Proc Natl Acad Sci U S A 1998;95:15542–6.
14. Wang MX, Kandiah DA, Ichikawa K, Khamashta M, Hughes G, Koike T, et al. Epitope specificity of monoclonal anti-β_2-glycoprotein I antibodies derived from patients with the antiphospholipid syndrome. J Immunol 1995;155:1629–36.
15. Atsumi T, Tsutsumi A, Amengual O, Khamashta MA, Hughes GR, Miyoshi Y, et al. Correlation between β_2-glycoprotein I valine/leucine^{247} polymorphism and anti-β_2-glycoprotein I antibodies in patients with primary antiphospholipid syndrome. Rheumatology (Oxford) 1999;38:721–3.
16. Matsuura E, Igarashi Y, Fujimoto M, Ichikawa K, Suzuki T, Sumida T, et al. Heterogeneity of anticardiolipin antibodies defined by the anticardiolipin cofactor. J Immunol 1992;148:3885–91.
17. Atsumi T, Ieko M, Bertolaccini ML, Ichikawa K, Tsutsumi A, Matsuura E, et al. Association of autoantibodies against the phosphatidylserine-prothrombin complex with manifestations of the antiphospholipid syndrome and with the presence of lupus anticoagulant. Arthritis Rheum 2000;43:1982–93.
18. Wilson WA, Gharavi AE, Koike T, Lockshin MD, Branch DW, Piette JC, et al. International consensus statement on preliminary classification criteria for definite antiphospholipid syndrome: report of an international workshop. Arthritis Rheum 1999;42:1309–11.
19. Tan EM, Cohen AS, Fries JF, Masi AT, McShane DJ, Rothfield NF, et al. The 1982 revised criteria for the classification of systemic lupus erythematosus. Arthritis Rheum 1982;25:1271–7.
20. Ichikawa K, Khamashta MA, Koike T, Matsuura E, Hughes GR. β_2-glycoprotein I reactivity of monoclonal anticardiolipin antibodies from patients with antiphospholipid syndrome. Arthritis Rheum 1994;37:1453–61.
21. Matsuura E, Igarashi M, Igarashi Y, Nagae H, Ichikawa K, Yasuda T, et al. Molecular definition of human β_2-glycoprotein I (β_2-GPI) by cDNA cloning and inter-species differences of β_2-GPI in alternation of anticardiolipin binding. Int Immunol 1991;3:1217–21.
22. Matsuura E, Igarashi Y, Yasuda T, Triplett DA, Koike T. Anticardiolipin antibodies recognize β_2-glycoprotein I structure altered by interacting with an oxygen modified solid phase surface. J Exp Med 1994;179:457–62.
23. Bouma B, de Groot PG, van den Elsen JM, Ravelli RB, Schouten A, Simmelink MJ, et al. Adhesion mechanism of human β_2-glycoprotein I to phospholipids based on its crystal structure. EMBO J 1999;18:5166–74.
24. Brooks BR, Bruccoleri RE, Olafson BD, States DJ. CHARMm: a program for macromolecular energy, minimization, and dynamics calculations. J Comput Chem 1983;4:187–217.
25. Carlson W, Karplus M, Haber E. Construction of a model for the three-dimensional structure of human renal renin. Hypertension 1985;7:13–26.
26. Hirose N, Williams R, Alberts AR, Furie RA, Chartash EK, Jain RI, et al. A role for the polymorphism at position 247 of the β_2-glycoprotein I gene in the generation of anti-β_2-glycoprotein I antibodies in the antiphospholipid syndrome. Arthritis Rheum 1999;42:1655–61.
27. Prieto GA, Cabral AR, Zapata-Zuñiga M, Simón AJ, Villa AR, Alarcon-Segovia D, et al. Valine/valine genotype at position 247 of the β_2-glycoprotein I gene in Mexican patients with primary antiphospholipid syndrome: association with anti-β_2-glycoprotein I antibodies. Arthritis Rheum 2003;48:471–4.
28. Camilleri RS, Mackie IJ, Humphries SE, Machin SJ, Cohen H. Lack of association of β_2-glycoprotein I polymorphisms Val247Leu and Trp316Ser with antiphospholipid antibodies in patients with thrombosis and pregnancy complications. Br J Haematol 2003;120:1066–72.
29. Ichikawa K, Tsutsumi A, Atsumi T, Matsuura E, Kobayashi S, Hughes GR, et al. A chimeric antibody with the human γ1 constant region as a putative standard for assays to detect IgG β_2-glycoprotein I-dependent anticardiolipin and anti-β_2-glycoprotein I antibodies. Arthritis Rheum 1999;42:2461–70.
30. Tincani A, Spatola L, Prati E, Allegri F, Ferremi P, Cattaneo R, et al. The anti-β_2-glycoprotein I activity in human anti-phospholipid syndrome sera is due to monoreactive low-affinity autoantibodies directed to epitopes located on native β_2-glycoprotein I and preserved during species' evolution. J Immunol 1996;157:5732–8.
31. Saxena A, Gries A, Schwarzenbacher R, Kostner GM, Laggner P, Prassl R. Crystallization and preliminary x-ray crystallographic studies on apolipoprotein H (β_2-glycoprotein-I) from human plasma. Acta Crystallogr D Biol Crystallogr 1998;54:1450–2.
32. Ito H, Matsushita S, Tokano Y, Nishimura H, Tanaka Y, Fujisao S, et al. Analysis of T cell responses to the β_2-glycoprotein I-derived peptide library in patients with anti-β_2-glycoprotein I antibody-associated autoimmunity. Hum Immunol 2000;61:366–77.
33. Arai T, Yoshida K, Kaburagi J, Inoko H, Ikeda Y, Kawakami Y, et al. Autoreactive CD4+ T-cell clones to β_2-glycoprotein I in patients with antiphospholipid syndrome: preferential recognition of the major phospholipid-binding site. Blood 2001;98:1889–96.

Human Molecular Genetics, 2004, Vol. 13, No. 2 *171–179*
DOI: 10.1093/hmg/ddh020

Gain-of-function polymorphism in mouse and human *Ltk*: implications for the pathogenesis of systemic lupus erythematosus

Na Li[1], Kazuhiro Nakamura[1], Yi Jiang[1,2], Hiromichi Tsurui[1], Shuji Matsuoka[1], Masaaki Abe[1], Mareki Ohtsuji[1], Hiroyuki Nishimura[3], Kiyoshi Kato[3,4], Takako Kawai[4], Tatsuya Atsumi[5], Takao Koike[5], Toshikazu Shirai[1,†], Hiroo Ueno[6] and Sachiko Hirose[1,*]

[1]Second Department of Pathology, Juntendo University School of Medicine, Tokyo 113-8421, Japan, [2]Central Laboratory of First Clinical College, China Medical University, Shenyang, People's Republic of China, [3]Toin Human Science and Technology Center, Department of Biomedical Engineering, Toin University of Yokohama, Yokohama 225-8502, Japan, [4]Department of Internal Medicine, Yokohama Seamen's Insurance Hospital, Yokohama 240-8585, Japan, [5]Second Department of Internal Medicine, Hokkaido University School of Medicine, Sapporo 060-8648, Japan and [6]Virology Division, National Cancer Center Research Institute, Tokyo 104-0045, Japan

Received August 19, 2003; Revised and Accepted November 11, 2003

Systemic lupus erythematosus (SLE), a complex multigenic disease, is a typical antibody-mediated autoimmune disease characterized by production of autoantibodies against a variety of autoantigens and immune complex-type tissue inflammation, most prominently in the kidney. Evidence suggests that genetic factors predisposing to aberrant proliferation/maturation of self-reactive B cells initiate and propagate the disease. In SLE-prone New Zealand Black (NZB) mice and their F_1 cross with New Zealand White (NZW) mice, B cell abnormalities can be ascribed mainly to self-reactive $CD5^+$ B1 cells. Our genome-wide scans to search for susceptibility genes for aberrant activation of B1 cells in these mice showed evidence that the gene, *Ltk*, encoding leukocyte tyrosine kinase (LTK), is a possible candidate. LTK is a receptor-type protein tyrosine kinase, belonging to the insulin receptor superfamily, and is mainly expressed in B lymphocyte precursors and neuronal tissues. Sequence and functional analyses of the gene revealed that NZB has a gain-of-function polymorphism in the LTK kinase domain near YXXM, a binding motif of the p85 subunit of phosphatidylinositol 3-kinase (PI3K). SLE patients also had this type of *Ltk* polymorphism with a significantly higher frequency compared with the healthy controls. Our findings suggest that these polymorphic LTKs cause up-regulation of the PI3K pathway and possibly form one genetic component of susceptibility to abnormal proliferation of self-reactive B cells in SLE.

INTRODUCTION

Systemic lupus erythematosus (SLE) is a complex multigenic disease (1). Clinical manifestations are extremely diverse and variable, mainly because of variable combinations of contributing genes at multiple loci in individual patients. Genes that predispose to SLE are undoubtedly related to key events in pathogenesis and involve a variety of genes in the immune system. Identification of such susceptibility alleles is hampered mainly because of difficulties in precisely determining SLE-associated immunological abnormalities in genetic studies. In this respect, related studies on animal models are valuable and may contribute to studies on identification of genes underlying basic immunoregulatory abnormalities of autoreactive lymphocytes in the pathogenesis of SLE (2).

New Zealand Black (NZB) mice spontaneously develop a mild form of immune complex-type glomerulonephritis later in life, in association with IgM hypergammaglobulinemia, including anti-DNA antibodies. Like NZB mice, the F_1 hybrid of the NZB and the non-autoimmune New Zealand White

*To whom correspondence should be addressed at: Second Department of Pathology, Juntendo University School of Medicine, 2-1-1, Hongo, Bunkyo-ku, Tokyo 113-8421, Japan. Tel: +81 358021039; Fax: +81 338133164; Email: sacchi@med.juntendo.ac.jp
†Emeritus Professor.

(NZW) mice have IgM hypergammaglobulinemia early in life. Unlike NZB, however, (NZB × NZW) F_1 mice develop florid SLE with a much earlier onset and with a higher incidence of renal disease, in parallel with antibody class switch from IgM to IgG when the animals are about 6 months of age (3). Thus, NZB genes determine disease phenotype and NZW genes augment the disease severity.

Much evidence supports the notion that the majority of early B cell abnormalities found in young NZB and (NZB × NZW) F_1 mice can be ascribed to $CD5^+$ B1 cells (4–6). Currently, at least two subpopulations, B1 and B2 cells, can be divided on the basis of differences in phenotype, physiology and antibody repertoire (7). Compared with conventional B2 cells that mainly participate in acquired immunity, B1 cells mainly participate in innate immunity, and produce IgM natural antibodies of a low-avidity nature, which are polyreactive and cross-react with a variety of self-antigens (8,9).

To determine the genes responsible for the aberrant activation of B1 cells, we did a genome-wide quantitative trait loci (QTL) analysis in (NZB × NZW) F_1 × NZB back-cross mice. One major susceptibility allele was mapped to the close vicinity of *Ltk*, the gene for leukocyte tyrosine kinase (LTK) on chromosome 2. The sequence analysis revealed that there is an amino acid substitution in the kinase domain of LTK in NZB mice. This type of polymorphism was also detected in human LTK, and the frequency of this polymorphic allele was significantly higher in patients with SLE compared with healthy controls. The possible involvement of the polymorphic *Ltk* alleles in susceptibility to SLE was examined by functional assays using transfected cells with constructs harboring the two different *Ltk* alleles.

RESULTS

Mapping of susceptibility loci for aberrant proliferation of peripheral B1 cells

Among 6-month-old NZB, NZW and (NZB × NZW) F_1 mice, NZB showed the highest frequency of peripheral $CD5^+$ B1 cells per total B cells, in association with IgM hypergammaglobulinemia. NZW showed the lowest frequency of B1 cells and the lowest serum IgM level, and (NZB × NZW) F_1 showed the intermediate phenotypes between NZB and NZW, suggesting that the contribution of the NZB-derived genes is co-dominant in these two phenotypes (Fig. 1).

To map NZB-derived susceptibility loci for the increased frequency of B1 cells, we did genome-wide scans for quantitative trait loci (QTL), using 261 (NZB × NZW) F_1 × NZB back-cross mice. The result revealed one NZB-derived region near the microsatellite marker, *D2Mit254*, on the middle part of chromosome 2 with significantly linkage (LOD 3.56 at *D2Mit254*; Fig. 2A). No other NZB-derived regions showed linkage to B1 cell frequency with at least suggestive linkage.

Sequence polymorphism in *Ltk* gene in the NZB mouse

Several genes, including *Ltk*, *Plcb2*, *Tyro3* and *B2m*, are located near *D2Mit254*, based on the MGI database (Fig. 2A).

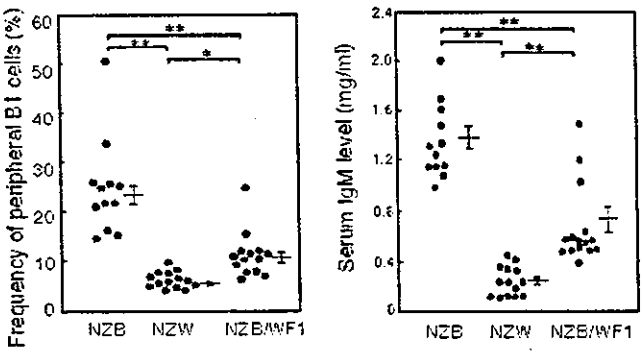

Figure 1. Comparisons of frequencies of peripheral $CD5^+$ B1 cells per total B cells and of serum IgM levels between NZB, NZW and (NZB × NZW) F_1 mice at 6 months of age. Each spot depicts data on an individual mouse, and mean ± SE is shown on the right. Asterisks indicate statistical significance ($^{**}P < 0.0002$; $^{*}P < 0.002$).

Among those, we focused on *Ltk*, because LTK was shown to be mainly expressed in B lineage cells (10). To examine *Ltk* as a candidate gene, the nucleotide sequence of *Ltk* was compared between NZB and NZW mice. The NZW sequence was the same as the reported one (10) and the BALB/c sequence (data not shown); however, there was a single nucleotide polymorphism (SNP) in NZB mice with A, instead of G, at position 1517. The deduced amino acid substitution is glutamic acid for glycine at position 746 in the kinase domain (Fig. 2B). With genotyping of back-cross mice for this SNP using PCR-SSCP (Fig. 2C), the LOD score for the increased frequency of B1 cells reached 4.80 (over 4.17, the threshold for highly significant linkage by permutation test) at the *Ltk* locus, thereby suggesting that *Ltk* is a strong candidate (Fig. 2A). Linkage of the *Ltk* locus with serum IgM levels was also significant (LOD 3.13), based on the permutation test (over 3.11, the threshold for significant linkage).

Sequence polymorphism in the *Ltk* gene in human SLE

To determine if the *Ltk* polymorphism is also associated with human SLE, PCR-SSCP was done using genomic DNA extracted from SLE patients and from healthy controls with primers covering the human LTK kinase domain corresponding to the mouse polymorphic region. Eleven of 151 patients (7.3%) and 16 of 575 healthy individuals (2.8%) were heterozygous for amplified region (Fig. 3A), and the heterozygous genotype frequency was significantly higher in the SLE patients compared to the case in healthy controls ($\chi^2 = 6.77$, $P = 0.009$). The nucleotide sequence revealed that individuals with homozygous alleles have G at position 9465, corresponding with glutamic acid at position 763 in the kinase domain. Those with heterozygous polymorphic alleles have both G and A at position 9465, corresponding with glutamic acid and lysine, respectively, at position 763 (Fig. 3B). Allele frequencies of 763K were 3.6 and 1.4% in SLE patients and controls, respectively, and the difference was statistically significant ($\chi^2 = 6.64$, $P = 0.01$). The odds ratio for the development of

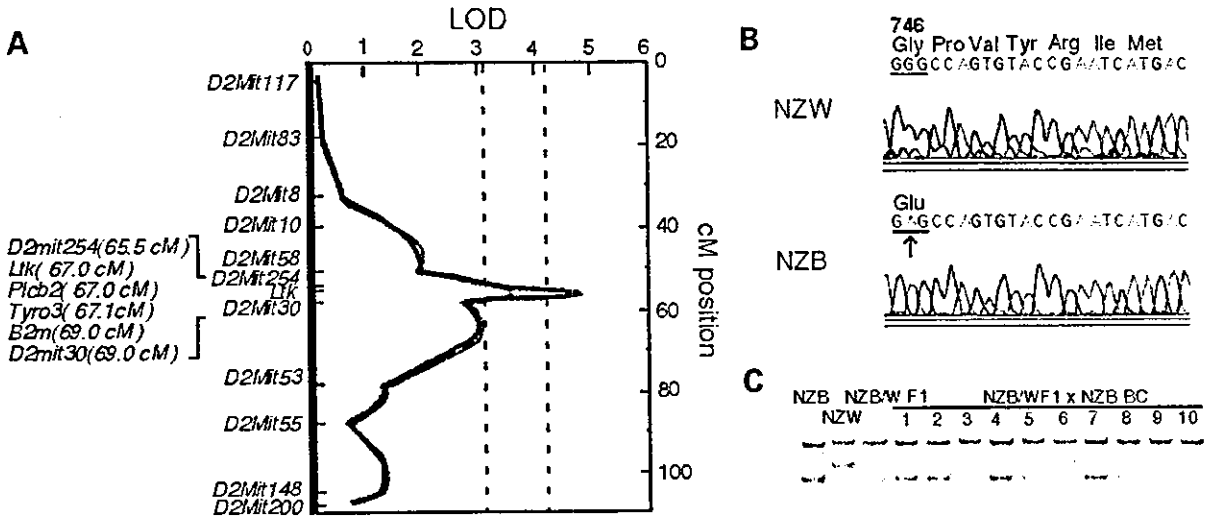

Figure 2. Linkage analysis of B1 cell frequency and SNP in *Ltk* in the NZB mouse. (**A**) Quantitative trait loci analysis of peripheral B1 cell frequency in total B cells in 261 (NZB × NZW) F_1 × NZB back-cross mice aged 6 months. Linkage was detected at the vicinity of *Ltk* on NZB chromosome 2. Blue and red lines show the result, with or without genotyping for *Ltk* SNP. Threshold for significant (LOD 3.08) and highly significant (LOD 4.17) linkage was based on the result of 1000 permutation test. Map positions of flanking microsatellite markers and genes are shown based on the MGI database. (**B**) Sequence analysis of *Ltk* cDNA from NZB and NZW mice. The NZB mouse had a G-A substitution (arrow), in association with glycine-glutamic acid substitution at codon 746 in the kinase domain (Fig. 4A). (**C**) PCR–SSCP for *Ltk* SNP in NZB, NZW, (NZB × NZW) F_1 and (NZB × NZW) F_1 × NZB back-cross mice. Primers for PCR were designed to amplify fragments encompassing SNP. Each NZB and NZW had two unique bands, and (NZB × NZW) F_1 mouse had the combined band pattern. In back-cross mice, nos 1, 2, 4 and 7 are NZB/NZB-type and nos 3, 5, 6, 8, 9 and 10 are NZB/NZW-type of *Ltk* genotype.

SLE with the 763E/K genotype versus the 763E/E genotype was 2.75 (95% CI 1.24–6.04).

Effects of polymorphic *Ltk* allele on kinase activity and p85 binding

Functional analyses of human LTK revealed that LTK is involved in the process of cell proliferation and survival, in which tyrosine 485, 753 and 862 contribute to specific binding with insulin receptor substrate-1 (IRS-1), p85 regulatory subunit of PI3K and Shc, respectively (11–13) (Fig. 4A). The observed amino acid substitution in NZB *Ltk* and human *Ltk*9465A allele is situated three amino acids upstream and 10 amino acids downstream from the tyrosine residue of p85-binding YXXM motif, respectively. Considering the importance of this region for the function of LTK, we examined the effect of the polymorphic alleles on the LTK activity. As the deduced protein sequence of LTK kinase domain shows 90% homology between mouse and human (14), we introduced NZB-type (750E) or human *Ltk*9465A-type (763K) substitution onto the *Ltk*9465G-type human *Ltk* allele (Fig. 4A), and the efficiency of autophosphorylation and the amount of p85 binding were examined, using COS7 cells transfected with these polymorphic *Ltk* alleles. Consistent with reported data (15), the capacity to catalyze autophosphorylation could still be observed in the *Ltk*9465G-type LTK in the absence of ligands. The extent of autophosphorylation was increased in both NZB-type and *Ltk*9465A-type LTK. The effect was more prominent in NZB-type substitution (Fig. 4B). These findings paralleled to extent of p85 binding (Fig. 4C), suggesting that both 750E and 763K variants enhance recruitment of PI3K to the cell membrane, resulting in activation of the PI3K pathway.

Effects of polymorphic *Ltk* allele on cell proliferation and survival

We then examined effects of 750E and 763K LTK variants on cell proliferation and survival. As no specific ligands for LTK have yet been identified, we took advantage of a chimeric receptor EL3 (hEGFR-hLTK) composed of an extracellular domain of human epidermal growth factor receptor (hEGFR) and transmembrane/cytoplasmic domains of human *Ltk*9465G-type LTK (hLTK) to analyze the function. The IL-3-dependent mouse pro-B cell line, Ba/F3 (16), was transfected with genes for the EL3 chimeric receptor (EL3 cells), or chimeric receptors with NZB-type (EL3-750E cells) or human *Ltk*9465A-type substitution (EL3-763K cells). Cells with the same expression levels of transfected genes were selected, using flow cytometry, and proliferative responses were compared with medium containing EGF in the absence of IL-3. The results of H^3-thymidine uptake showed a significant increase in both EL3-750E and EL3-763K compared with findings in EL3 cells. This increase was probably due to the up-regulated PI3K pathway, since the effect was abolished in the presence of a specific PI3K inhibitor, Ly294002 (Fig. 5A). Cell cycle analysis revealed a higher proportion of cells in the S/M phase and a lower proportion of apoptotic cells in EL3-750E than in EL3 cells (Fig. 5B), suggesting that the up-regulated PI3K pathway in EL3-750E cells contributes not only to cell proliferation but also to anti-apoptosis.

DISCUSSION

In the present studies, we carried out a genome-wide QTL analysis to search for susceptibility loci to the activation of self-reactive B1 cells seen in SLE-prone NZB and (NZB × NZW)

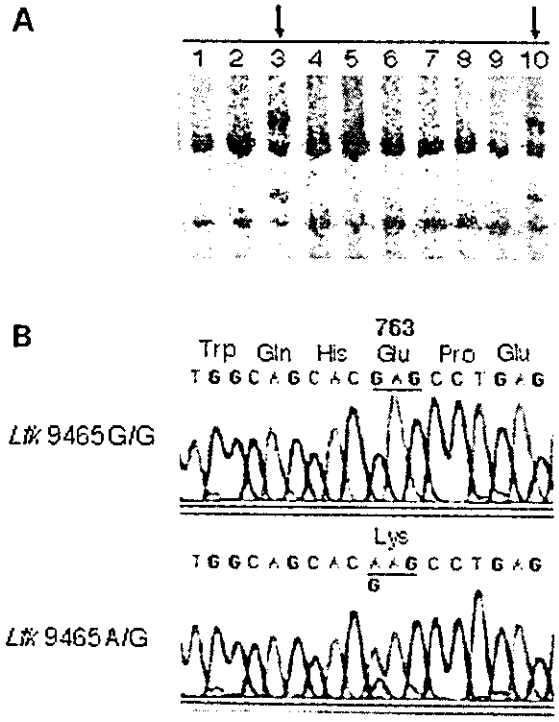

Figure 3. Polymorphism in human *Ltk*. (A) PCR–SSCP for detection of *Ltk* polymorphism. The results for 10 SLE patients are shown. Eleven of 151 SLE patients were heterozygous (shown by the arrow) for amplified *Ltk* fragment. Sixteen of 575 healthy controls were also heterozygous, but the heterozygous genotype frequency was significantly higher in SLE patients compared with controls ($\chi^2 = 6.77$, $P = 0.009$). Primers for PCR were designed to amplify the ~200 bp fragment corresponding to the mouse polymorphic region. (B) Direct sequence analysis of homozygous (*Ltk*9465G/G) and heterozygous (*Ltk*9465A/G) *Ltk* alleles. Heterozygous individuals had both G and A at position 9465, corresponding to glutamic acid and lysine at codon 763 in the kinase domain (Fig. 4A).

F_1 mice. We found that one NZB-derived allele located in the vicinity of *Ltk* on chromosome 2 was significantly linked to the increased frequency of B1 cells in conjunction with IgM hypergammaglobulinemia. Among several genes located in the vicinity of *Ltk*, such as *Plcb2*, *Tyro3* and *B2m* (MGI database), *Ltk* itself was thought to be a possible candidate for aberrant activation of self-reactive B cells, because LTK is preferentially expressed on B lineage cells, and because NZB has a gain-of-function polymorphism in LTK kinase domain.

LTK is a receptor-type protein tyrosine kinase, belonging to the insulin receptor family (10,17,18), and is mainly expressed in pre-B cells and brain (10). In previous studies, we found that human LTK utilizes two major signaling molecules, Shc, which binds to tyrosine 862 at the carboxyl-terminal domain, and IRS-1, which binds to tyrosine 485 at the juxtamembrane domain, and that both molecules stimulate growth signals transmitted through the Ras pathway (11,12). It was also noted that the p85 regulatory subunit of PI3K directly binds to tyrosine 753, which is located within a YXXM motif, a consensus binding amino acid sequence for the SH2 domain of p85, in the kinase domain of human LTK (13). The deduced amino acid sequence of mouse LTK kinase domain shows 90% homology to human LTK (14). The observed NZB-type amino acid substitution of glutamic acid for glycine is situated three amino acids upstream from the tyrosine residue in the YXXM motif. Our data suggest that NZB-type substitution enhances ligand-independent autophosphorylation of tyrosine residue in YXXM motif and recruitment of PI3K to the cell membrane through the up-regulated p85-binding, the result being activation of the PI3K pathway. It seems that an amino acid substitution of cationic lysine for anionic glutamic acid in human *Ltk*9464A-type allele can also increase autophosphorylation and p85 binding to a given extent.

The PI3K pathway is an important signaling cascade that regulates various cellular events, including cell proliferation and survival (19). Several recent studies using transgenic or gene knock out mice have linked the PI3K pathway with autoimmune susceptibility (20–22). Transgenic mice with T cell-specific expression of $p65^{PI3K}$, an active form of PI3K, or of protein kinase B (PKB), a downstream effector of PI3K, developed splenomegaly and lymphadenopathy, in association with increased serum immunoglobulin levels and widespread inflammation including autoimmune kidney disease (21,22). Thus, T cell-specific up-regulation of the PI3K/PKB pathway results in activation of not only T cells but also B cell populations. Analysis of T cells from these mice showed that they were resistant to Fas-mediated apoptosis. Furthermore, mice with heterozygous deletion of the phosphatase and tensin homologue (PTEN) gene ($PTEN^{+/-}$ mice) developed lymphoid hyperplasia composed of both T and B cells with hypergammaglobulinemia (20). PTEN was shown to negatively regulate PKB (23,24). Taken collectively, these studies show that enhanced activation of the PI3K/PKB pathway alters lymphocyte homeostasis and predisposes mice to autoimmunity (25). This is consistent with our idea that a gain-of-function polymorphism of LTK could form one aspect of the genetic susceptibility to SLE with altered autoreactive B cell homeostasis, through PI3K pathway activation.

Since LTK is expressed in immature B cells (10), one can speculate that frequencies of not only B1 cells but also B2 cells per total lymphocytes are linked to LTK gene polymorphism in our QTL analysis. However this was not the case, perhaps due to characteristic features of B1 cells. In contrast to conventional B2 cells, B1 cells have a self-replenishing capacity (7) and are constitutively stimulated by self-antigens via their self-reactive B cell receptors (26). Furthermore, B1, but not B2, cells in NZB and (NZB × NZW) F_1 mice are resistant to Fas-mediated activation-induced cell death (27). Thus, it seems likely that B1 cells in these mice are more sensitive to the altered activation levels of the PI3K pathway than are B2 cells. This notion is consistent with the finding that mice lacking the p110δ catalytic subunit of PI3K have a reduced number of B1 cells (28).

The occurrence of multigenic diseases such as SLE has been explained in a threshold liability model, in which individuals will develop disease when the effects of total numbers of disease susceptibility genes exceed a given threshold (29). Such multigenic control of SLE involves genetic heterogeneity, in which several independently segregating susceptibility loci control the same disease phenotype (30). In the present studies, 7.3% of SLE patients had the gain-of-function type polymorphic *Ltk* allele. It is possible that many other unexplored molecules may be involved in abnormal activation of

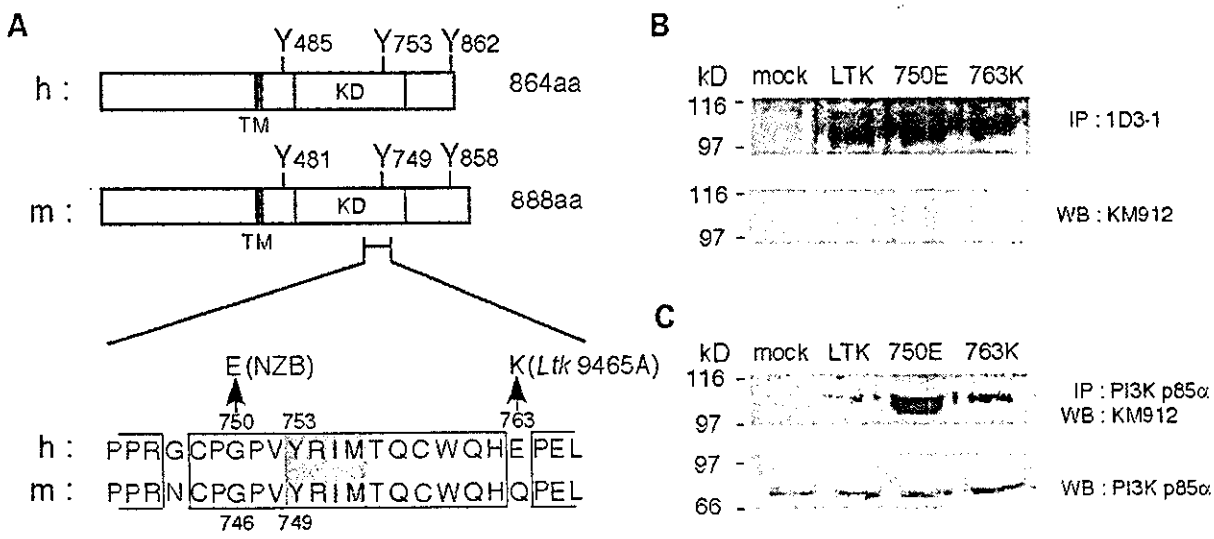

Figure 4. Amino acid substitutions in the kinase domains of NZB-type and human *Ltk*9465A-type LTK, and up-regulated effects on autophosphorylation and P85 binding. (**A**) Schematic structure of human (h) and mouse (m) LTK of the full-sized isoform (TM, transmembrane domain, KD, kinase domain). Partial amino acid sequences around p85-binding YXXM motif (shown in gray) are given below. Identical amino acid between human and mouse are boxed. Amino acid substitutions in NZB-type and human *Ltk*9465A-type LTK were indicated. (**B**) *In vitro* kinase assay in human *Ltk*9465G-type LTK (LTK), human LTKs with NZB-type (750E) and human LTKs with *Ltk*9465A-type substitution (763K). Cell lysate of COS7 cells transfected with vector alone (mock) or each *Ltk* construct was immunoprecipitated with mAb against the intracellular domain of LTK (1D3-1), and incubated with [γ-P^{32}] ATP, followed by SDS–PAGE and autoradiography. A representative result of three independent experiments is shown. Relative radioactivities of phosphorylated bands in LTK, 750E and 763K were 1, 1.42 ± 0.14 and 1.37 ± 0.12, respectively, and the difference in activity between LTK and 750E was statistically significant ($P < 0.01$). The lower panel shows the control for the amount of LTK protein applied using western blotting with mAb KM912, specific for the extracellular domain of LTK. A marker of molecular mass is shown on the left. (**C**) Comparison of amounts of p85 binding. The cell lysate was immunoprecipitated with antibody against PI3Kp85α, and subjected to SDS–PAGE, followed by blotting with mAb KM912. A representative result in three independent experiments is shown. The lower panel shows the control for the amount of p85 protein applied using western blotting with antibody against PI3Kp85α.

autoreactive B cells. Notably, 2.8% of healthy controls also had the same polymorphic *Ltk* allele, undoubtedly indicating that this type of LTK variant *per se* is insufficient to develop SLE. In this context, NZB mice only develop a mild form of SLE, and NZW-derived genetic factors, one of which is linked to NZW major histocompatibility complex (MHC) (reviewed in 2), are essential for the severe form of SLE associated with IgM to IgG class switch of autoantibodies observed in (NZB × NZW) F_1 mice. The association between human SLE and HLA-DR2 and DR3 has also been shown in many studies in Caucasian populations. In addition to MHC, cumulative evidence supports several gene variants conferring predisposition to SLE (reviewed in 1), such as genes encoding classical complement components, low affinity receptors for IgG and PDCD1 (31). In SLE mouse models, several chromosomal segments have shown the association with disease phenotypes (reviewed in 32), and possible involvement of several gene variants, such as *Cd22* (33), *Cr2* (34), *Ifi202* (35). *C1q* (36) and *Fcgr2b* (37), has been described. Different combinations of these and not yet identified genetic variants may contribute to SLE susceptibility in different cohorts.

The human LTK gene lies in 15q15.1–15q21.1 (LocusLink database, Locus ID 4058). A genome-wide search for susceptibility genes in SLE sib-pair analysis showed suggestive linkages between SLE and microsatellite markers located at 15q15.1 on chromosome 15 (38). There is a large variation among studied samples in size, ethnic composition and family structure (1). Thus, further genetic studies in different cohorts and different races will be needed to confirm the linkage with marker loci in 15q15.1–15q21.1 and LTK polymorphism. Based on studies in both murine models and human SLE, a wider knowledge and a more thorough understanding of the genetic mechanisms of SLE are expected to provide clues as to the pathogenesis, then prophylactic and therapeutic clinical approaches can be better designed.

MATERIALS AND METHODS

Mice and subjects

NZB, NZW and (NZB × NZW) F_1 mice obtained from Shizuoka Laboratory Animal Center (Shizuoka, Japan) were maintained in our laboratory. Back-cross mice were obtained by crossing female (NZB × NZW) F_1 mice with male NZB mice. In human studies, 19 autopsy cases and 132 patients with SLE were analyzed. The patients were diagnosed according to the American College of Rheumatology criteria for SLE (39). The SLE group consisted of 18 male patients and 133 female patients at ages ranging from 22 to 81 years (mean ± SD = 42.7 ± 12.5). The apparently healthy control group consisted of researchers, laboratory workers, and students (183 men and 392 women) at ages ranging from 11 to 98 years (mean ± SD = 47.8 ± 21.8). All subjects were of the Japanese race, and relatively homozygous with respect to genetic background, permitting the case–control approach used in this study. The study was reviewed and approved by the research ethics committee.

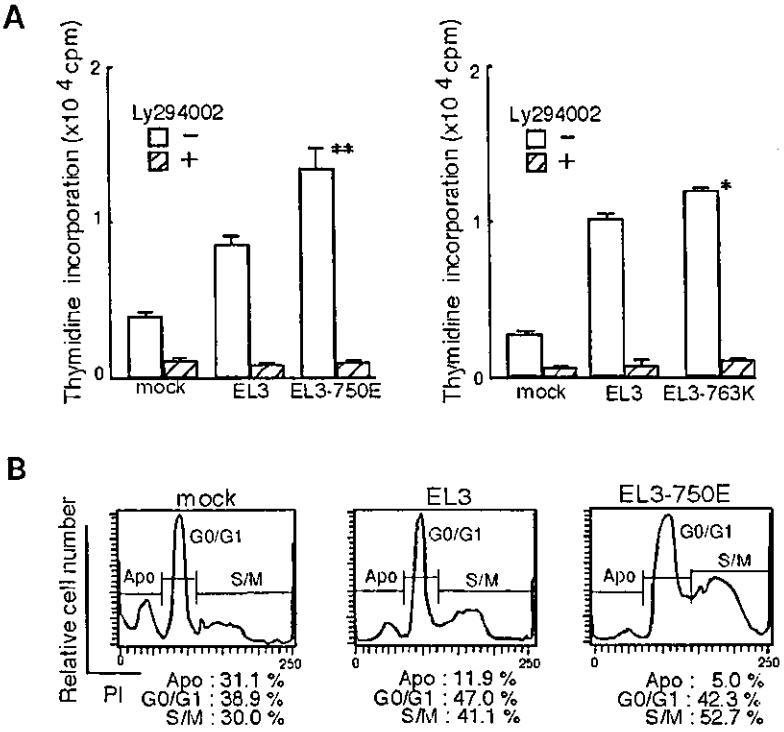

Figure 5. Effects of NZB-type and human *Ltk*9465A-type LTK on proliferation and survival in Ba/F3 transfectants. (**A**) Ba/F3 cells were transfected with vector alone (mock), hEGFR-hLTK chimeric receptor (EL3) or chimeric receptor with NZB-type (EL3-750E) or human *Ltk*9465A-type *Ltk* (EL3-763K). These cells were incubated with EGF for 16 h, with or without Ly294002, a specific inhibitor of PI3K, in the presence of [H^3] thymidine during the final 3 h, and the uptake of [H^3] thymidine was compared. The experiments were done in four independent wells and mean and SE are shown. Asterisks indicate statistical significance compared to EL3 cells (**$P < 0.005$; *$P < 0.01$). (**B**) Cell cycle analysis in mock, EL3 and EL3-750E cells. Starved cells were stimulated with EGF for 16 h, fixed with 70% ethanol and incubated with propidium iodine (PI). Frequencies of cells in apoptosis (Apo), G0/G1 phase and S/M phase were calculated using flow cytometry. A representative profile of a histogram for the intensity of PI staining in four independent experiments is shown. The mean and SE of Apo frequencies in mock, EL3 and EL3-750E cells were 44.1 ± 5.7, 21.5 ± 9.6 and 8.4 ± 3.4%, respectively, and the difference between EL3 and EL3-750E was statistically significant ($P < 0.05$).

Flow cytometry for peripheral B cell subset

Peripheral blood was obtained from periorbital sinuses of mice, followed by lysis of red blood cells using ammonium chloride. Cells were then incubated with FITC-labeled rat anti-mouse CD5 monoclonal antibody (mAb; clone 53-7.3) and biotinylated rat anti-mouse CD45R (B220) mAb (clone RA3-6B2), followed by phycoerythrin (PE)–avidin (Becton-Dickinson, Mountain View, CA, USA), and examined using FACStar (Becton Dickinson).

Genotyping and PCR-SSCP

DNA was extracted from the mouse-tail. Genotyping was done using microsatellite markers (Research Genetics, Hunteville, AL, USA) distributed approximately every 10 cM over the entire genome, except for the sex chromosome. PCR was done in a three-temperature protocol (94, 58 and 72°C) for 45 cycles using a GeneAmp 9600 Thermal Cycler (Perkin-Elmer Applied Biosystems, Foster City, CA, USA). PCR products were run on 18% polyacrylamide gels and visualized after ethidium bromide staining. For genotyping of *Ltk* SNP, PCR-SSCP was done using primers designed to amplify fragments encompassing nucleotide substitution at position 1517. The 5′ and 3′ primers used were 5′-TCATTGCCACAGGGAACAGG-3′ (1472–1491) and 5′-TCAGGGTCCTGAGTGCAGTA-3′ (1603–1622), respectively. After the initial denaturation at 95°C for 5 min, PCR was done in a three-temperature protocol (95, 55 and 72°C) for 40 cycles, using GeneAmp reagents and AmpliTaq Gold DNA polymerase (Perkin-Elmer Applied Biosystems). PCR products were denaturated at 98°C for 10 min, immediately cooled on ice, and run on a 10% polyacrylamide gel with 5% glycerol in 0.5 × TBE buffer under a constant current at 24°C for 2 h. Single-stranded DNA fragments in the gel were visualized with use of silver staining.

For PCR–SSCP analysis for human samples, genomic DNA was extracted from peripheral blood leukocytes from patients with SLE and control subjects, or kidney samples of autopsied patients, using a standard method. Primers were designed to amplify fragments encompassing nucleotide substitution at position 9465. PCR was done with radiolabeled forward primer 5′-TGGACTTCGTCGTTGGAGGA-3′ (9301–9320) and unlabeled reverse primer 5′-CAAGATGCTGGCAAAGCTAG-3′ (9481–9500), and amplified products were electrophoresed on a 5% polyacrylamide gel with 10% glycerol in 1 × TBE buffer overnight in 5 W at 4°C. Autoradiograms were obtained using the BAS 2500 (Bio Imaging System, Fuji Film, Tokyo, Japan).

Nucleotide and amino acid sequences and positions are based on the following database. Mouse *Ltk* cDNA, GenBank X52621; mouse LTK, swissprot P08923; human *Ltk* genomic DNA, GenBank NM_002344; human LTK, swissprot P29376.

Statistics

The linkage of a particular locus with peripheral B1 cell frequency in total B cells was examined in 261 (NZB × NZW) F_1 × NZB back-cross mice, using a computer package program of Map Manager/QTL. LOD score over 1.9 and 3.3 was used as thresholds for statistically suggestive and significant linkage, respectively, according to Lander and Kruglyak (40). Permutation test was also done for estimating the statistical significance. Differences in genotype and allele frequencies in SLE patients and non-SLE controls were compared using chi-square test. The odds ratio and its 95% confidence interval (95% CI) were calculated to provide an estimate of the risk of SLE in a given *Ltk* genotype compared with the controls. Differences in B1 cell frequencies, serum IgM levels, intensity of LTK autophosphorylation, thymidine incorporation and apoptotic cell frequencies were estimated using Student's *t*-test. The *P*-value <0.05 was considered statistically significant.

Sequencing

For the mouse *Ltk* sequence, first-stranded cDNA was synthesized from bone marrow-derived total RNA using an oligo(dT) primer and the 2181 bp *Ltk* gene was amplified using appropriate primer pairs, referred to the database (GenBank X52621). For partial sequence of human *Ltk* in genomic DNA, PCR products of position 9227–9726 (corresponding to Serine 708–Proline 818) were amplified using appropriate primers, referred to the database (GenBank NM_002344). The PCR products were isolated using agarose gel electrophoresis, then both strands were directly sequenced using the dideoxy chain termination method with *Taq* dye primer cycle sequencing kits (Perkin-Elmer Applied Biosystems).

Plasmid construction and *in vitro* mutagenesis

cDNAs of the hLTK (*Ltk*9465G haplotype) and the chimeric receptor EL3 (hEGFR-hLTK), were subcloned into expression vector pUC-CAGGS and pSRαMSVtk*neo*, respectively, and used as templates for site-directed mutagenesis, as described (11). We used the two-step PCR-based method (41) to introduce a single nucleotide substitution in *Ltk*9465G cDNA. The first PCR was done with primers, 5′-CC TAGGGGCTGCCCAGAGCCTGTGTACCGC-3′and 5′-GC GGTACACAGGCTCTGGGCAGCCCCTAGG-3′, for the substitution of glutamic acid for glycine at position 750 (NZB-type: 750E), and with primers, 5′-CAGTGTTGGC AGCACAAGCCTGAGCTCCGC-3′and 5′-GCGGAGCTC AGGCTTGTGCTGCCAACACTG-3′, for substitution of lysine for glutamic acid at position 763 (human *Ltk*9465A-haplotype: 763K). The nucleotides to be substituted are underlined. The second PCR was done with the common flanking primers, 5′-TCTTTTGGGGTGCTGCTCTGG-3′ and 5′-TGGGGGTCTTAGGCACTCTAA-3′. The PCR fragments carrying substitutions were cut with *Bgl*II and ligated into h*Ltk*–pUC-CAGGS or *EL3*–pSRαMSVtk*neo* at the corresponding *Bgl*II-digested portion. Introduction of substitutions was verified by sequencing.

In vitro kinase assay and p85 binding assay

COS7 cells were transfected with h*Ltk*–pUC-CAGGS with or without substitutions, using the DEAE–dextran method. For the LTK kinase assay, cell lysates containing total protein of 700 μg in Tris–HCl lysis buffer (0.5%, Triton X-100, 50 mM Tris–HCl, pH 7.4, 2 mM PMSF, 1 mM sodium orthovanadate, 1 mM EDTA, 10 units/ml aprotinin) were incubated with protein A-Sepharose coated by 1D3-1, a mouse mAb recognizing the intracellular domain of hLTK (42), for 1 h at 4°C, followed by three washes with wash buffer (0.1%, Triton X-100, 50 mM Tris–HCl, pH 7.4) and once with kinase buffer (40 mM HEPES, pH 7.4, 10 mM $MgCl_2$, 3 mM $MnCl_2$). The immunoprecipitates were incubated with 10 μCi [γ-P^{32}] ATP for 20 min at room temperature, and the reactions were analyzed using 7.5% SDS–PAGE and autoradiography.

For the P85 binding assay, cell lysates containing a total of 15 mg protein were immunoprecipitated with Z-8, polyclonal rabbit antibody against PI3Kp85α subunit, (Santa Cruz Biotech, Santa Cruz, CA, USA), and subjected to 7.5% gel SDS–PAGE. The immunoblotting was done with KM912, a mouse mAb recognizing the extracellular domain of human LTK (42).

For control of LTK or p85 protein levels in the kinase assay and p85-binding assay, cell lysates containing total of 50 μg protein were subjected to 7.5% gel SDS–PAGE. Western blotting was done with KM912 or Z-8, followed by alkaline phosphatase-conjugated goat anti-mouse or -rabbit IgG antibody (CAPPEL, West Chester, PA, USA). The color reaction was done using BCIP/NBT Color Development Substrate (Promega, Madison, WI, USA).

Cell proliferation and cell cycle assays

To examine the effects of amino acid substitutions on cellular function in the LTK kinase domain, Ba/F3 cells were transfected with cDNAs of EL3, EL3-750E or EL3-763K using the retrovirus vector (pSRαMSVtk*neo*), as described (12). To determine the cell proliferation, cells with the same expression level of transfected genes were selected using flow cytometry with Ab-1, a mouse mAb specific for the extracellular domain of hEGFR (Oncogene Science, Cambridge, MA, USA), and the [H^3] thymidine incorporation assay was done. In 96-well plates 10^4cells/well were cultured in starvation medium (RPMI1640 containing 0.5% FCS, but not mouse IL-3) for 6 h, then incubated with or without 25 μM of Ly294002 (Sigma, St Louis, MO, USA), a specific PI3K inhibitor, for 30 min. The cells were then stimulated with 50 ng/ml of EGF (WAKUNAGA, Hiroshima, Japan) for 16 h in the presence of 0.5 μCi of [H^3] thymidine during the final 3 h and were subjected to liquid scintillation measurements of radioactivity.

For cell cycle analysis, a final density of 1×10^5 cells/ml in 10 cm dish was cultured in starvation medium for 6 h. After incubation with 50 ng/ml of EGF for 16 h, cells were fixed with 70% ice-cold ethanol for 30 min, followed by treatment with

500 μg/ml of RNaseA (Roche, Indiana, IN, USA) at 37°C for 20 min. Then cells were incubated with 50 μg/ml of propidium iodide (PI; Sigma) at 4°C for 30 min, and were analyzed using FACStar and the CellQuest software.

ACKNOWLEDGEMENTS

We thank Dr Andre Bernards (Harvard Medical School, Boston, MA, USA) and Dr Hisamaru Hirai (Graduate School of Medicine, University of Tokyo, Japan) for kind help with mouse and human *Ltk* experiments, respectively. We also thank M. Ohara (Fukuoka, Japan) for language assistance. This work was supported by Grant-in-Aid for Scientific Research (B) and for Scientific Research on Priority Areas from the Ministry of Education, Science, Technology, Sports and Culture, Japan.

REFERENCES

1. Tsao, B.P. (2002) The genetics of human lupus. In Wallace, D.J. and Hahn, B.H. (eds), *Dubois' Lupus Erythematosus*, 6th edn. Lippincott Williams & Wilkins, Philadelphia, PA, pp. 97–119.
2. Hirose, H., Jiang, Y., Hamano, Y. and Shirai, T. (2000) Genetics aspects of inherent B-cell abnormalities associated with SLE and B-cell malignancy: lessons from New Zealand mouse models. *Int. Rev. Immunol.*, **19**, 389–421.
3. Shirai, T., Hirose, S., Okada, T. and Nishimura, H. (1991) Immunology and immunopathology of the autoimmune disease of NZB and related mouse strains. In Rihova, B. and Vetvicka, V. (eds). *Immunological Disorders in Mice*. CRC Press, Boca Raton, FL, pp. 95–136.
4. Hasegawa, K., Abe, M., Okada, T., Hirose, S., Sato, H. and Shirai, T. (1989) Are Ly-1 B cells responsible for the IL2-hyperresponsiveness of B cells in autoimmune-prone NZB × NZW F_1 mice? *Int. Immunol.*, **1**, 99–103.
5. Abe, M., Okada, T., Matsumoto, K., Ishida, Y., Shiota, J., Nishimura, H., Hirose, S., Sato, H. and Shirai, T. (1989) The novel murine B cell differentiation antigen Lp-3. *Int. Immunol.*, **1**, 576–581.
6. Kanno, K., Okada, T., Abe, M., Hirose, S. and Shirai, T. (1993) Differential sensitivity to interleukins of $CD5^+$ and $CD5^-$ anti-DNA antibody-producing B cells in murine lupus. *Autoimmunity*, **14**, 205–214.
7. Herzenberg, L.A., Kantor, A.B. and Herzenberg, L.A. (1992) Layered evolution in the immune system. A model for the ontogeny and development of multiple lymphocyte lineages. *Ann. NY Acad. Sci.*, **651**, 1–9.
8. Kocks, C. and Rajewsky, K. (1989) Stable expression and somatic hypermutation of antibody V regions in B-cell developmental pathways. *A. Rev. Immunol.*, **7**, 537–559.
9. Casali, P. and Notkins, A.L. (1989) $CD5^+$ B lymphocytes, polyreactive antibodies and the human B-cell repertoire. *Immunol. Today*, **10**, 364–368.
10. Bernards, A. and de la Monte, S.M. (1990) The ltk receptor tyrosine kinase is expressed in pre-B lymphocytes and cerebral neurons and uses a non-AUG translational initiator. *EMBO J.*, **9**, 2279–2287.
11. Ueno, H., Hirano, N., Kozutsumi, H., Sasaki, K., Tanaka, T., Yazaki, Y. and Hirai, H. (1995) An epidermal growth factor receptor-leukocyte tyrosine kinase chimeric receptor generates ligand-dependent growth signals through the Ras signaling pathway. *J. Biol. Chem.*, **270**, 20135–20142.
12. Ueno, H., Sasaki, K., Kozutsumi, H., Miyagawa, K., Mitani, K., Yazaki, Y. and Hirai, H. (1996) Growth and survival signals transmitted via two distinct NPXY motifs within leukocyte tyrosine kinase, an insulin receptor-related tyrosine kinase. *J. Biol. Chem.*, **271**, 27707–27714.
13. Ueno, H., Honda, H., Nakamoto, T., Yamagata, T., Sasaki, K., Miyagawa, K., Mitani, K., Yazaki, Y. and Hirai, H. (1997) The phosphatidylinositol 3′ kinase pathway is required for the survival signal of leukocyte tyrosine kinase. *Oncogene*, **14**, 3067–3072.
14. Maru, Y., Hirai, H. and Takaku, F. (1990) human *ltk* gene structure and preferential expression in human leukemic cells. *Oncogene Res.*, **5**, 199–204.
15. Kozutsumi, H., Toyoshima, H., Hagiwara, K., Furuya, A., Mioh, H., Hanai, N., Yazaki, Y. and Hirai, H. (1993) Identification of the *ltk* gene product in placenta and hematopoietic cell lines. *Biochem. Biophys. Res. Commun.*, **190**, 674–679.
16. Palacios, R. and Steinmetz, M. (1985) Il-3-dependent mouse clones that express B-220 surface antigen, contain Ig genes in germ-line configuration, and generate B lymphocytes *in vivo*. *Cell*, **41**, 727–734.
17. Ben-Neriah, Y. and Bauskin, A.R. (1988) Leukocytes express a novel gene encoding a putative transmembrane protein-kinase devoid of an extra-cellular domain. *Nature*, **333**, 672–676.
18. Krolewski, J.J. and Dalla-Favera, R. (1991) The ltk gene encodes a novel receptor-type protein tyrosine kinase. *EMBO J.*, **10**, 2911–2919.
19. Chan, T.O., Rittenhouse, S.E. and Tsichlis, P.N. (1999) AKT/PKB and other D3 phosphoinositide-regulated kinases: kinase activation by phosphoinositide-dependent phosphorylation. *A. Rev. Biochem.*, **68**, 965–1014.
20. Di Cristofano, A., Kotsi, P., Peng, Y.F., Cordon-Cardo, C., Elkon, K.B. and Pandolfi, P.P. (1999) Impaired Fas response and autoimmunity in $Pten^{+/-}$ mice. *Science*, **285**, 2122–2125.
21. Borlado, L.R., Redondo, C., Alvarez, B., Jimenez, C., Criado, L.M., Flores, J., Marcos, M.A.R., Martinez-A, C., Balomenos, D. and Carrera, A.C. (2000) Increased phosphoinositide 3-kinase activity induces a lymphoproliferative disorder and contributes to tumor generation *in vivo*. *FASEB J.*, **14**, 895–903.
22. Parsons, M.J., Jones, R.G., Tsao, M-S., Odermatt, B., Ohashi, P.S. and Woodgett, J.R. (2001) Expression of active protein kinase B in T cells perturbs both T and B cell homeostasis and promotes inflammation. *J. Immunol.*, **167**, 42–48.
23. Maehama, T. and Dixon, J.E. (1998) The tumor suppressor, PTEN/MMAC1, dephosphorylates the lipid second messenger, phosphatidylinositol-3,4,5-triphosphate. *J. Biol. Chem.*, **273**, 13375–13378.
24. Stambolic, V., Suzuki, A., de la Pompa, J.L., Brothers, G.M., Mirtsos, C., Sasaki, T., Ruland, J., Penninger, J.M., Siderovski, D.P. and Mak, T.W. (1998) Negative regulation of PKB/Akt-dependent cell survival by the tumor suppressor PTEN. *Cell*, **95**, 29–39.
25. Ohashi, P.S. (2002) T-cell signalling and autoimmunity: molecular mechanisms of disease. *Nat. Rev. Immunol.*, **2**, 427–438.
26. Hayakawa, K., Asano, M., Shinton, S.A., Gui, M., Allman, D., Stewart, C.L., Silver, J. and Hardy, R.R. (1999) Positive selection of natural autoreactive B cells. *Science*, **285**, 113–116.
27. Hirose, S., Yan, K., Abe, M., Jiang, Y., Hamano, Y., Tsurui, H. and Shirai, T. (1997) Precursor B cells for autoantibody production in genomically Fas-intact autoimmune disease are not subject to Fas-mediated immune elimination. *Proc. Natl Acad. Sci. USA*, **94**, 9291–9295.
28. Clayton, E., Bardi, G., Bell, S.E., Chantry, D., Downes, C.P., Gray, A., Humphries, L.A., Rawlings, D., Reynolds, H., Vigorito, E. *et al.* (2002) A crucial role for the p110δ subunit of phosphatidylinositol 3-kinase in B cell development and activation. *J. Exp. Med.*, **196**, 753–763.
29. Nishimura, H. and Ozaki, S. (2000) Practical approaches to determining disease-susceptibility loci in multigenic autoimmune models. *Int. Rev. Immunol.*, **19**, 335–366.
30. Wandstrat, A. and Wakeland, E. (2001) The genetics of complex autoimmune diseases: non-MHC susceptibility genes. *Nat. Immunol.*, **2**, 802–809.
31. Prokunina, L., Castillejo-Lopez, C., Oberg, F., Gunnarsson, I., Berg, L., Magnusson, V., Brookes, A.J., Tentler, D., Kristjansdottir, H., Grondal, G. *et al.* (2002) A regulatory polymorphism in *PDCD1* is associated with susceptibility to systemic lupus erythematosus in humans. *Nat. Genet.*, **32**, 666–669.
32. Shirai, T., Nishimura, H., Jiang, Y. and Hirose, S. (2002) Genome screening for susceptibility loci in systemic lupus erythematosus. *Am. J. Pharmacogen.*, **2**, 1–12.
33. Lajaunias, F., Ibnou-Zekri, N., Jimack, L.F., Chicheportiche, Y., Parkhouse, R.M.E., Mary, C., Reininger, L., Brighouse, G. and Izui, S. (1999) polymorphisms in the *Cd22* gene of inbred mouse strains. *Immunogenetics*, **49**, 991–995.
34. Boackle, S.A., Holers, V.M., Chen, X., Szakonyi, G., Krap, D.R., Wakeland, E.K. and Morel, L. (2001) *Cr2*, a candidate gene in the murine *Sle1c* lupus susceptibility locus, encodes a dysfunctional protein. *Immunity*, **15**, 775–785.
35. Rozzo, S.J., Allard, J.D., Choubey, D., Vyse, T.J., Izui, S., Peltz, G. and Kotzin, B.L. (2001) Evidence for an interferon-inducible gene, *Ifi202*, in the susceptibility to systemic lupus. *Immunity*, **15**, 435–443.
36. Miura-Shimura, Y., Nakamura, K., Ohtsuji, M., Tomita, H., Jiang, Y., Abe, M., Zhang, D., Hamano, Y., Tsuda, H., Hashimoto, H. *et al.* (2002) *C1q* regulatory region polymorphism down-regulating murine C1q protein levels with linkage to lupus nephritis. *J. Immunol.*, **169**, 1334–1339.

37. Xie, Y., Nakamura, K., Abe, M., Li, N., Wen, X-S., Jiang, Y., Zhang, D., Tsurui, H., Matsuoka, S., Hamano, Y. *et al.* (2002) Transcriptional regulation of *Fcgr2b* gene by polymorphic promoter region and its contribution to humoral immune responses. *J. Immunol.*, **169**, 4340–4346.
38. Rao, S., Olson, J.M., Moser, K.L., Gray-McGuire, C., Bruner, G.R., Kelly, J. and Harley, J.B. (2001) Linkage analysis of human systemic lupus erythematosus-related traits. A principal component approach. *Arthritis Rheum.*, **44**, 2807–2818.
39. Tan, E.M., Cohen, A.S., Fires, J.F., Masi, A.T., McShane D.J., Rothfield, N.F., Schaller, J.G., Talal, N. and Winchester, R.J. (1982) The 1982 revised criteria for the classification of systemic lupus erythematosus. *Arthritis Rheum.*, **25**, 1271–1277.
40. Lander, E. and Kruglyak, L. (1995) Genetic dissection of complex traits: guideline for interpreting and reporting linkage results. *Nat. Genet.*, **11**, 241–247.
41. Li, S. and Wilkinson, M.F. (1997) Site-directed mutagenesis: a two-step method using PCR and *Dpn*I. *BioTechniques*, **23**, 588–590.
42. Toyoshima, H., Kozutsumi, H., Maru, Y., Hagiwara, K., Furuya, A., Mioh, H., Hanai, N., Takaku, F., Yazaki, Y. and Hirai, H. (1993) Differently spliced cDNAs of human leukocyte tyrosine receptor tyrosine kinase predict receptor protein with and without a tyrosine kinase domain and a soluble receptor protein. *Proc. Natl Acad. Sci. USA*, **90**, 5404–5408.

Reprinted from JOURNAL OF NEUROLOGY, NEUROSURGERY & PSYCHIATRY, January 2004, Vol 75, No1, p 140

NEUROLOGICAL PICTURE

Double pituitary adenomas with distinct histological features and immunophenotypes

We present a case of double pituitary adenomas with distinct pathological features. A 59 year old Japanese woman was referred to Hokkaido University Hospital for endocrinological examination of acromegaly. The patient showed typical acromegalic features. Growth hormone (GH) and insulin-like growth factor 1 were 17.1 ng/ml and 1620 ng/ml, respectively. Other pituitary hormones including thyroid stimulating hormone (TSH), prolactin, gonadotropins, and adrenocorticotropic hormone (ACTH) were within normal ranges. GH was not suppressed in the 75 g oral glucose tolerance test. Although the response of TSH was normal, GH showed a paradoxical rise to 200 μg with thyrotropin releasing hormone administration. On imaging analysis, double low intensity regions separated by a normal pituitary were identified (fig 1). Based on the diagnosis of acromegaly, transsphenoidal pituitary adenomectomy was done. Each tumour showed distinct histological and immunohistochemical features; the left adenoma consisted of relatively small cells with hyperchromatic nuclei immunoreactive for TSH. In contrast, the tumour cells of the right tumour were acidophilic and cytoplasm rich with an intense immunoreactivity for GH (fig 2). Other pituitary hormones including luteinising hormone, follicle stimulating hormone, prolactin, and ACTH were immunohistochemically negative for both adenomas.

The incidence of double or multiple pituitary adenomas is approximately 1% of autopsy pituitaries[1] and 0.4% to 1.3% of a surgically resected series.[2 3] In the present case, one adenoma was endocrinologically active but the other inactive regardless of being immunohistochemically positive for TSH. The independent production of distinct pituitary hormones from each adenoma has been reported,[2] so one should take into consideration doing an intensive preoperative imaging analysis if one hopes to accomplish complete remission of endocrinopathy.

Figure 1 (A) Coronal T1 weighted MR image revealing a suprasellar extension on the right side of the pituitary complex. (B) Gadolinium enhanced coronal T1 weighted MR image indicating two hypointense lesions, clearly separated by a well enhanced normal pituitary.

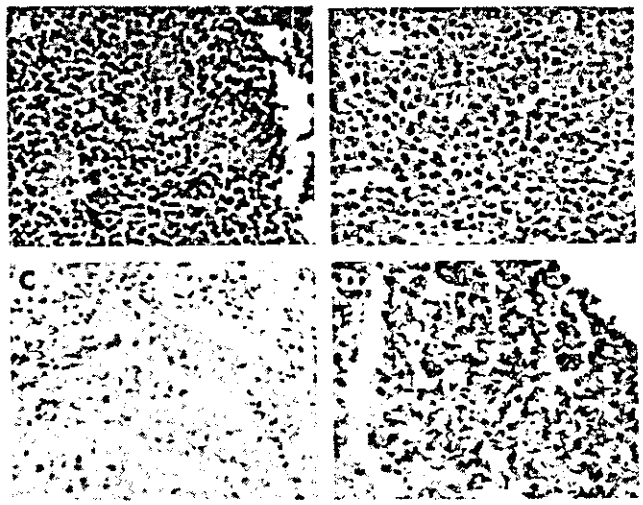

Figure 2 (A) Hematoxylin eosin staining showing relatively small cells in the adenoma left. A rosette like pattern with spindle shaped cells is evident (arrowheads). (B) The right sided tumour was composed of strongly acidophilic, more cellular, adenomatous cells with a diffuse pattern of cell growth. (C) Immunohistochemistry revealing immunoreactivity for thyroid stimulating hormone in the adenoma on the left. (D) Immunohistochemistry revealing immunoreactivity for growth hormone in the other on the right.

Acknowledgement

This work was supported in part by a Grant-in-Aid for Research on Specific Diseases "Hypothalamo-Pituitary Dysfunction" from the Ministry of Health, Labour and Welfare, Japan.

C Shimizu, T Koike
Division of Clinical Endocrinology and Metabolism, Department of Medicine II, Hokkaido University Graduate School of Medicine
Y Sawamura
Department of Neurosurgery, Hokkaido University Graduate School of Medicine

Correspondence to: Dr C Shimizu; Department of Medicine II, Hokkaido University Graduate School of Medicine, N-15 W-7, Kita-ku, Sapporo 060-8638, Japan; shimizch@med.hokudai.ac.jp

References

1 **Kontogeorgos G**, Kovacs K, Horvath E, *et al.* Multiple adenomas of the human pituitary. A retrospective autopsy study with clinical implications. *J Neurosurg* 1991;74:243–7.
2 **Kontogeorgos G**, Scheithauer BW, Horvath E, *et al.* Double adenomas of the pituitary. A clinicopathological study of 11 tumors. *Neurosurg* 1992;31:840–9.
3 **Sano T**, Horiguchi H, Xu B, *et al.* Double pituitary adenomas: Six surgical cases. *Pituitary* 1999;1:243–50.

Ann Hematol (2004) 83:114-116
DOI 10.1007/s00277-003-0740-z

CASE REPORT

T. Endo · S. Nakao · K. Koizumi · M. Nishio · K. Fujimoto · T. Sakai · K. Kumano · M. Obara · T. Koike

Successful treatment with rituximab for autoimmune hemolytic anemia concomitant with proliferation of Epstein-Barr virus and monoclonal gammopathy in a post-nonmyeloablative stem cell transplant patient

Received: 12 May 2003 / Accepted: 10 July 2003 / Published online: 25 September 2003

Abstract A 30-year-old Japanese woman who underwent nonmyeloablative stem cell transplantation from her HLA-matched sister developed autoimmune hemolytic anemia (AIHA). There was proliferation of EBV-DNA in her peripheral blood and monoclonal gammopathy, both predictive factors of post-transplant lymphoproliferative disorder (PTLD). As conventional immunosuppressive therapy for AIHA could lead to overt PTLD, we decided to give her rituximab 375 mg/m^2 once weekly for a total of four doses. After this therapy, both her AIHA and monoclonal gammopathy were resolved and EBV-DNA became undetectable. Rituximab therapy deserves consideration for treatment of post-allogeneic stem cell transplant patients with AIHA, especially for patients who cannot be given immunosuppressive therapy.

Keywords Autoimmune hemolytic anemia (AIHA) · Monoclonal gammopathy · Epstein-Barr virus (EBV) · Rituximab · Post-transplant lymphoproliferative disorder (PTLD)

Introduction

Autoimmune hemolytic anemia (AIHA) is a relatively common disorder seen by hematologists. The first line treatment is usually immunosuppressive therapy such as corticosteroids, cyclophosphamide and azathioprine and most patients respond to this therapy. AIHA can occur in the setting of post-allogeneic stem cell transplantation (SCT) [2, 3]. However, AIHA following allogeneic-SCT is often difficult to treat and the overall prognosis is poor [3]. Immunosuppressive therapy could complicate an already existing immune deficiency and these patients are put at risk for infectious complications; in fact many patients died with infectious complications or AIHA [3, 8].

Post-transplant lymphoproliferative disorder (PTLD) is also one of the serious complications of SCT [11, 15]. Generally, it is induced by Epstein-Barr Virus (EBV) in severely immunocompromised patients. Once PTLD becomes distinct, the prognosis is poor, and mortality rates can reach up to 90% [6, 11]. Thus pre-emptive treatment should be based on predictive factors of PTLD such as an elevated EBV viral load and development of monoclonal gammopathy [1, 4]. In such cases, reduction of immunosuppressive agents is a first-line therapeutic approach [10].

As stated above, approved therapeutic approaches to AIHA and PTLD are contrary to each other, so it is difficult to treat when these two diseases are concomitant. We describe here effective treatment with rituximab, a highly specific mouse/human chimeric anti-CD20 antibody, for AIHA concomitant with proliferation of EBV and monoclonal gammopathy in a post-non-myeloablative stem cell transplant patient.

T. Endo (✉) · K. Koizumi · M. Nishio · K. Fujimoto · T. Sakai · K. Kumano · M. Obara · T. Koike
Department of Internal Medicine II,
Hokkaido University School of Medicine,
N-15, W-7, Kita-ku, 060-8638 Sapporo, Hokkaido, Japan
e-mail: t-endo@fd5.so-net.ne.jp
Tel.: +81-11-7065915
Fax: +81-11-7067710

S. Nakao
Third Department of Medicine,
Kanazawa University School of Medicine, Kanazawa, Japan

Case report

A 30-year-old Japanese woman with severe aplastic anemia diagnosed 20 years earlier underwent non-myeloablative allogeneic peripheral blood stem cell transplantation (PBSCT) from her HLA-matched sister in September 2000 [9]. Both donor and recipient